Earth and Planetary Science Letters 568 (2021) 117035

Contents lists available at ScienceDirect

Earth and Planetary Science Letters

www.elsevier.com/locate/epsl

Resolving the argument about volcanic bedrock under the West Antarctic Ice Sheet and implications for ice sheet stability and sea level change

John T. Andrews [a,*], Wesley LeMasurier [b]

[a] Department of Geological Sciences and INSTAAR, University of Colorado, Boulder, CO 80303, United States of America
[b] INSTAAR, University of Colorado, Boulder, CO 80303, United States of America

ARTICLE INFO

Article history:
Received 24 November 2020
Received in revised form 10 May 2021
Accepted 1 June 2021
Available online 15 June 2021
Editor: J.P. Avouac

Keywords:
Antarctic bedrock
Cenozoic volcanics
Ross Sea mineral composition
sediment unmixing
glacial erosion

ABSTRACT

We provide a test for recent arguments that the West Antarctic Ice Sheet (WAIS) is underlain by an extensive outcrop of volcanic rock (mainly basalt) by examining the non-clay and clay mineral composition of sediments collected in front of and under the Ross Ice Shelf. If the proposed large volume were present, then we posit that glacial erosion and transport would deliver sediments to the Ross Sea enriched in minerals diagnostic of alkaline basalt, namely olivine, pyroxene, and plagioclase, and no quartz. Using quantitative X-ray diffraction analysis, we determine the weight percent of minerals in West Antarctic alkaline basalt, dolerite, gneiss, and granite bedrock, and compare these with a suite of 49 surface and near-surface sediment samples from a 1400 km west to east transect across the Ross Sea. Fifty percent of the samples had quartz percentage values >25% and had very small wt percentages of diagnostic basalt minerals. A sediment unmixing algorithm, with basalt, dolerite, gneiss and granite bedrock, end members, showed that the sediment contained virtually no basalt, was dominated by granite compositions, but did show some samples with an admixture of material derived from the Ferrar dolerite, which crops out extensively in the Transantarctic Mountains. Indicators of possible late Cenozoic volcanic bedrock – pyroxene, forsterite, and smectite weight percentages – decrease from west to east across the Ross Sea opposite to the trend of the quartz weight percent. Our study provides no support for the presence of extensive basalt outcrop under the WAIS, hence indicates that any changes in ice stream stability will not be influenced by basal heat regime.

1. Introduction

Within the past 2-3 decades several studies have raised the specter of a renewal of subglacial volcanic activity, that would further destabilize the West Antarctic Ice Sheet (WAIS) beyond the instability inherent in the fact that the ice is grounded well below sea level (Hughes, 1975; Mercer, 1978) and buttressed from collapse by ice, that are currently undergoing significant reduction (Depoorter et al., 2013; Wellner et al., 2019). Behrendt et al. (1993) proposed the existence of "at least 10^6 km^3 of probable late Cenozoic volcanic rock" beneath the WAIS, and the Ross ice shelf, in the West Antarctic rift system (WARS). This was based on a >100,000 km widely spaced aeromagnetic survey that revealed numerous semi-circular, high amplitude magnetic anomalies. In the Ross Sea itself, eight seismically defined structures that penetrate the sedimentary section are associated with short-wavelength magnetic anomalies. These also have been interpreted as volcanic in origin (Behrendt, 1990; Behrendt et al., 1993). Blankenship et al. (1993) proposed the existence of an active "Casertz" volcano near the southern boundary of the rift system (Fig. 1) based on an aeromagnetic survey that revealed a large amplitude, long-wavelength magnetic anomaly located over a 6 km wide, 650 m high subglacial peak which lies below a "distinct depression" in the ice sheet surface. Corr and Vaughan (2008) used radar data to identify a subglacial tephra layer with an area of roughly 23,000 km^2 within the Pliocene – Quaternary Hudson Mountains volcanic field, which lies on the east side of Pine Island glacier (Fig. 1). The estimated volume of ash implies an explosivity index of 3-4 (Mt. St. Helens was a 5), and its depth in the ice implies an age of 207 BC ± 240 yr. They infer that the episodic release of water during such an eruption "probably affected ice flow" in this already vulnerable part of the WAIS.

* Corresponding author.
E-mail addresses: andrewsj@colorado.edu (J.T. Andrews), wesley.lemasurier@colorado.edu (W. LeMasurier).

https://doi.org/10.1016/j.epsl.2021.117035
0012-821X/

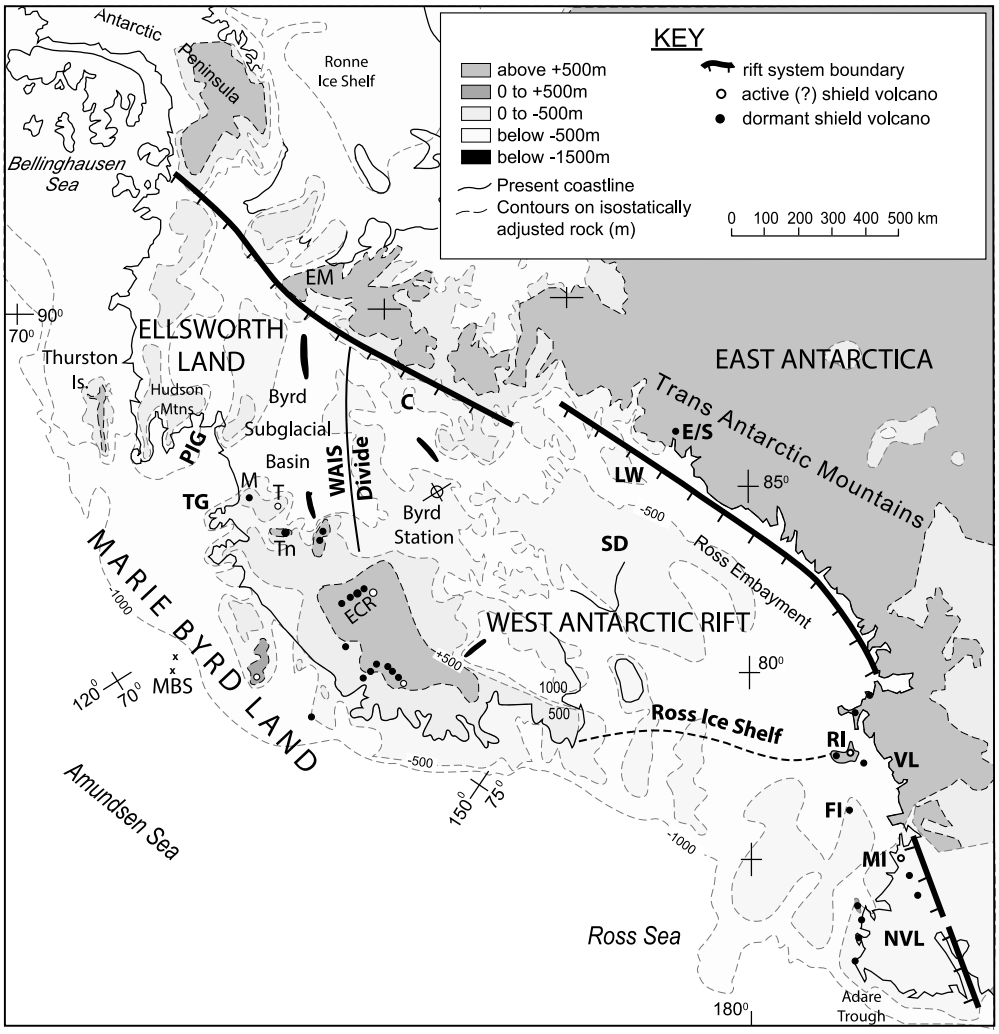

Fig. 1. Index map of the West Antarctic rift system. The WAIS Divide separates the portion of the West Antarctic ice sheet (WAIS) that flows into the Ross Sea from that portion which flows into the Amundsen and Bellingshausen Seas. The MBL volcanic province includes, and is defined by, all the shield volcanoes shown. Isostatically adjusted ice-free bedrock topography is simplified from Drewry (1983). Abbreviations: C, Casertz subglacial volcano; ECR, Executive Committee Range; EM, Ellsworth Mountains; E/S, Mt. Early/Sheridan Bluff volcanoes; FI, Franklin Island; LW, Lake Whillans; M, Mt. Murphy; MBS, Marie Byrd Seamounts; MI, Mt. Melbourne; NVL, Northern Victoria Land; PIG, Pine Island Glacier; RI, Ross Island; SD, SipleDome; T, Mt. Takahe; TG, Thwaites Glacier; Tn, Toney Mtn; VL, Victoria Land. Greenwich meridian is up, following the convention for small scale maps of Antarctica.

Recently, Van Wyk De Vries et al. (2017) used ice bed elevation data to locate conical edifices that protrude upward into the ice sheet across the West Antarctic rift. Based on these morphometric data, and the assumption that all cones are volcanic in origin, and the association of the cones with concentric magnetic anomalies, they identified 138 "volcanoes" concentrated along the ~3000 km central axis of the rift system. They range from 6 km to 58 km in diameter and 100 m to 3850 m in height above the surrounded bedrock floor. On this basis they define a new subglacial volcanic province.

Our study provides a geologic test for the existence of large volumes of subglacial volcanic rock, possibly of late Cenozoic age, and by inference, the potential for a destabilizing volcanic eruption. We believe that if the large volume of volcanic rock inferred from these studies truly exists beneath the WAIS, then evidence for its' existence should be clearly present in the debris delivered to Ross Sea basins by the ice streams that head into the Ross Sea Ice Shelf, and we should be able to confirm or refute the claims put forward by these publications.

The primary result of glacial erosion is the production of silt and clay-sized sediments (Alley et al., 1997; Boulton, 1982, 1996; Dreimanis, 1976, 1984; Drewry, 1986; Dowdeswell and Scourse, 1990). The mineral and chemical products of glacial erosion are transported toward glacier termini and eventually released as suspended sediment in meltwater plumes or hyperpycnal flows (turbidity currents) (Kurtz and Anderson, 1979), or carried farther from the ice front as ice rafted debris (IRD) (Anderson et al., 1980, 1991; Bartek and Anderson, 1991). In Antarctica the ice streams are fronted by extensive ice shelves, and the sedimentological evidence (Anderson and Bartek, 1991; Anderson et al., 1991; Domack and Harris, 1998; Licht et al., 1999; McKay et al., 2016) shows that the sediment content of icebergs calved from the front of ice shelves is small, representing a limited rate of erosion. The transport of sediment under and away from the pervasive ice shelf (Wellner et al., 2019) is primarily in the form of fine-grained suspended sediment (McKay et al., 2016). In Canada the chemical and mineral signatures of glacial sediments have been used as a signature of specific bedrock for economic mineral purposes (Klassen, 1993; Shilts, 1976), and a broader array of provenance indicators have been utilized for paleo-glacial and –oceanographic reconstructions in the North Atlantic and around Antarctica including X-ray diffraction and radiogenic isotopes (Andrews and Tedesco, 1992; Farmer et al., 2003; Farmer and Licht, 2016; Hemming, 2004; Licht and Hemming, 2017; Licht et al., 2006). U-Pb

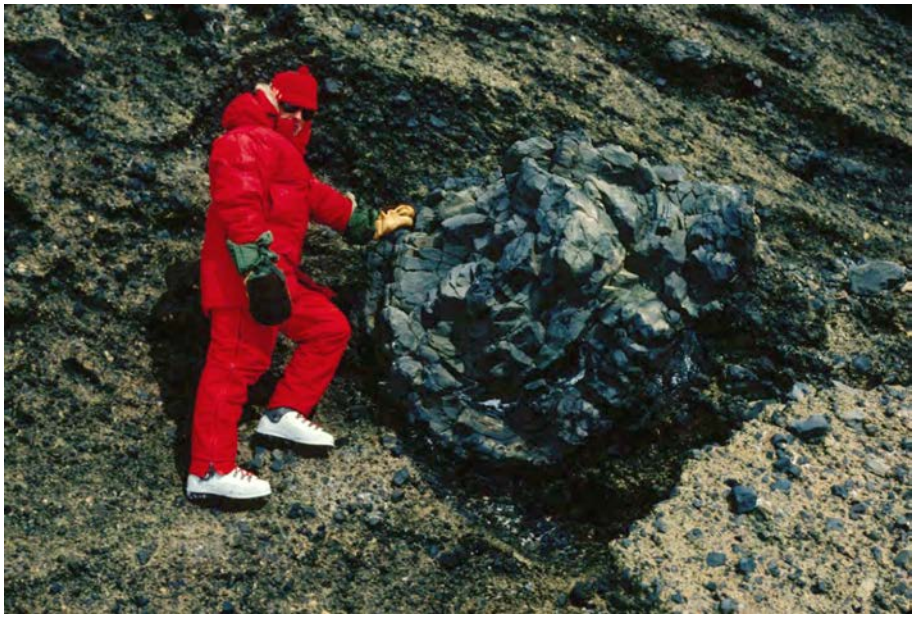

Fig. 2. Hyaloclastite tuff breccia, aka palagonite tuff breccia, from the base of Mt. Takahe, showing textures and structures commonly seen in these deposits. They are typically composed of a large proportion of volcanic ash, altered to the mineraloid palagonite, and include glass-rich lava clasts and globules all produced by rapid chilling and fragmentation during subglacial eruptions. Yellow material in this figure is palagonite, a hydrous alteration product of volcanic glass typically composed of clay minerals, zeolites, and Fe-oxides. The rounded globule and S-shaped bedding above the man's shoulder were produced by downslope flowage of water-saturated tuff breccia. Photo by W.E. LeMasurier.

detrital zircon ages have been used to define ice flow patterns in the Ross Sea embayment (Licht et al., 2014).

Our hypothesis: We argue that if there were extensive areas of Cenozoic volcanic rock under the WAIS, that glacial erosion and meltwater transport (Golledge et al., 2013; King et al., 2020) would result in characteristic volcanic minerals being a significant component of the sediment archive. Studies of exposed volcanoes in Marie Byrd Land (MBL) provide evidence that roughly 90% of Cenozoic volcanic rock is alkaline basalt (LeMasurier and Thomson, 1990; LeMasurier, 2013), hence we expect mafic minerals to be an important component of the volcanic debris. Furthermore, hyaloclastite tuff breccias have been shown to be easily eroded, even by cold-based polar ice (LeMasurier and Rocchi, 2005; Rocchi et al., 2006), which makes their representation in Ross Sea sediment cores even more likely, if indeed the ice sheet is underlain by a significant volume of these rocks. We test this hypothesis by examining 78 grab and core samples from the area of Ross Sea (Fig. 1A) and comparing their mineral compositions with West Antarctic bedrock samples of alkaline basalt, Ferrar dolerite (from the Transantarctic Mountains only), gneiss, and granite. As a comparison we provide data on the mineral composition of glacial marine sediments seaward of the East Greenland 60,000 km^2 early Tertiary basalt outcrop (Brooks and Nielsen, 1982; Larsen, 1983). These sediments should be similar in composition to Ross Sea sediments, if indeed there are $\sim 10^6$ km^3 of late Cenozoic alkali basalts concealed beneath the WAIS.

2. Bedrock geology

On a regional scale, the late Cenozoic volcanoes of West Antarctica rest on a complex Paleozoic-Mesozoic magmatic arc terrain that is everywhere dominated by calc-alkaline granitoids of Devonian, Permian, and Cretaceous ages. The most widespread of these are Early Cretaceous. These granitoids represent prolonged intervals of subduction along the Gondwanaland coast. The basement intruded by these rocks consists mainly of lower Paleozoic greenschist to amphibolite facies metaclastic and metavolcanic rocks and granitic orthogneisses.

The largest volume of exposed volcanic rock in West Antarctica is in the MBL province (Fig. 1). It includes 18 basalt-trachyte shield volcanoes with exposed volumes roughly in the range 400 km^3–1800 km^3, plus more than 30 small (<1 km^3) isolated basaltic centers (LeMasurier and Thomson, 1990). The total volume of volcanic cannot be estimated with any confidence, because most of the shield volcanoes are partially buried beneath the ice sheet, with usually just the felsic/intermediate summit sections exposed. However, the summit sections appear to be only $\sim$10% of the total volcano volume, as inferred from the best exposures of basal successions (LeMasurier, 2013). As an example, the one seismic traverse across the province revealed that an exposed 600 m section of basalt is underlain by an additional 4400 m beneath the ice, for a total of $\sim$5000 m of basalt underlying Toney Mountain volcano Bentley et al., 1974; LeMasurier and Thomson, 1990).

Where the bases of these volcanic sections are exposed, they are composed of hyaloclastites and pillow lavas, interbedded with tillites, and resting on glacially striated basement rock, clearly representing subglacial eruptions (Fig. 2). The lithologic character of these deposits determines the nature of the detritus we would expect to find in sea floor core samples. Pillow lavas typically are enclosed by a 5-6 cm rind of glass that sloughs off producing non-vesicular vitric clasts during eruption. Hyaloclastites typically occur in as chaotic breccia deposits that include lava globules and glass-rich clasts with a large range of sizes, in a matrix of yellow-brown palagonitized vitric ash (Fig. 2). The latter are rapidly altered in the hot, aqueous depositional environment to zeolites phillipsite, chabazite, and analcime, and smectite clay minerals (Ellerman, 1992).

Volcanologists will note that eruptions at the -500 m to -1000 m depths found in the interior of the rift system are more likely to produce pillow lavas than hyaloclastites, because hydrostatic pressure at those depths prevents both the explosive vesiculation and the explosive generation of steam that yield the classic Icelandic table mountain deposits (Jones, 1966, 1969). However, detailed studies of MBL hyaloclastites (LeMasurier, 2002) show that

they are, in all but one locality, composed of the blocky, non-vesicular clasts produced by non-explosive fragmentation, rather than the vesicular clasts bounded by concave bubble walls produced by shallow water explosive eruptions. In this regard, MBL hyaloclastites are much like those described by Honnorez and Kirst (1975), formed by vitrification and granulation during quenching in deep submarine environments, and by Clague et al. (2000) by lava fountaining at ~4200 m depths in the sea around Hawaii. It seems that hyaloclastites and pillow lavas are equally likely products of eruptions in the rift interior, and both would produce significant quantities of volcanic glass.

To the east and west of the MBL province, along the Pacific coast, Cenozoic volcanic exposures are almost entirely basaltic and relatively small, in some cases a single flow, and others up to ~500 m thicknesses of flows and hyaloclastite tuffs. It should also be noted that volcanic rocks similar to those in MBL are exposed along the western Ross Sea coast (the McMurdo Volcanic Group) in Victoria Land (LeMasurier and Thomson, 1990, Chapter A). Olivine and pyroxene in two cores from the western Ross Sea, adjacent to the coast, are undoubtedly derived from alkali basalt outcrops on this coast and are irrelevant to the question of whether large volumes of volcanic rock lie beneath the WAIS.

If a large volume of late Cenozoic volcanic rock is indeed present below the WAIS, we would expect basal heat flow to be relatively high. This is important because high values would be expected to impact basal melt-rates; but direct measurements of heat flow are difficult to make in ice-covered regions. Shapiro and Ritzwoller (2004) used a global seismic model of the crust and upper mantel to infer heat flow of ~80 mW/m^2 for our area of interest, decreasing to ~50 mW/m^2 toward the pole. The first direct measurements of heat flow were made by Fisher et al. (2015) from sediments below subglacial Lake Whillans (Fig. 1, LW). They recorded a value of 285 ± 80 mW/m^2, roughly equivalent to those at Yellowstone. More recently, Clow (unpublished data) has measured 104 mW/m^2 at the WAIS divide, and 65 mW/m^2 at Siple dome (Fig. 1). The continental average is 55 mW/m^2. The high variability of these results is similar to findings in other rift systems, where high values are typically found along rift faults, and low values away from faults (Clow, pers. comm.).

3. Quantitative X-ray diffraction of sediment mineralogy and sediment unmixing

We used the whole pattern approach of Eberl (2003) which was used to detect major differences in the contribution of the glacial erosion of basalt outcrops on the East versus West Precambrian granitoid margins of Greenland (Andrews et al., 2015). This approach to obtaining reliable estimates of mineral compositions of sediments placed second in the International Reynolds Cup competition (McCarty, 2002; Raven and Self, 2017), which requires laboratories to determine the percentages of non-clay and clay minerals in prepared sediment mixtures. In the Amundsen Sea embayment (Fig. 1). The accuracy and precision of different whole pattern Rockjock methods, using several prepared non-clay and clay mixtures, are documented in a Supplement to this paper. Ehrmann et al. (2011) have provided qualitative data on the clay mineral distributions (that is the sediment fraction <2 μm).

The method consists of weighing 1 g of the <2 mm sediment fraction (sand, silt, and clay), adding 10% by weight of zincite, grinding in a McCrone mill and drying. The intensity measurements are then processed in a macro-Excel program Rockjock v6, which contains standard patterns for 124 minerals. Rockjock v6 uses samples from the White River tephra (Alaska) as a standard for amorphous silica (glass). However, the whole XRD pattern signature of diatoms is very close to that of volcanic glass (Andrews et al., 2013) rendering a detailed interpretation of "amorphous silica" difficult. The qXRD results are reported as either mg/g or as a wt% and are normalized to sum to either 1 g or 100%. Variations in percentage values have to be evaluated judicially because of the closed array constraints (Aitchison, 1986; Chayes, 1971). Initially we estimate the weight %s of 20 non-clay and 10 clay minerals, including four alkali feldspars (ordered microcline to anorthoclase) and five plagioclase feldspars (albite to anorthite), but we then consolidate the minerals into 16 species, and use the combined wt% of K- and Na-feldspars, and Ca-feldspars, as well as combining the carbonate minerals, and various XRD patterns of illite (Table 1).

We use the program "SedUnMix" (Andrews and Eberl, 2012) to estimate the percent of bedrock contribution to the Ross Sea glacial marine sediment. Four West Antarctic bedrock sources were used, namely: alkali basalt, Ferrar dolerite (Transantarctic Mountains only), gneiss, and granites. Ideally the sum of the sources should sum to 100% but differences from this ideal give an indication of the extent of additional source(s) or processes. Amorphous is not present in any quantity in the bedrock source except the hyaloclastites, and neither is smectite. For the SedUnMix analyses we excluded volcanic glass; the program estimates a standard deviation of the estimates bedrock components by iteratively randomly sampling each of the bedrock types 100 times. The measure of the degree-of-fit (DOF) between the observed and calculated is: (sum of the absolute differences/100) (Andrews and Eberl, 2012), although a more intuitive measure is the average bias (AveB) (in this case: AveB = DOF*100/15).

3.1. West Antarctic bedrock mineral signatures

The most diagnostic minerals for our purposes, are quartz and forsterite. Virtually all of the pre-volcanic basement igneous and metasedimentary rocks are quartz-rich (Table 2, Fig. 3, Suppl. Table 1) whereas the Cenozoic volcanic rocks are largely quartz-free (e.g. in the entire MBL province, one rhyolite flow has been found with quartz phenocrysts (6.4%). To quantify the degree of association between bedrock and sample compositions (Table 2) we use the Similarity Coefficient (SC) (Sarna-Wojcicki et al., 1984), which has a range between 0 and 100%. It is a very sensitive measure as all mineral ratios have equal weight regardless of their wt% (thus 0.1 and 0.3 wt% have the same product as 10 and 30 wt%), We thus calculate SG (Table 2; Suppl. Table 1) for the non-clay and clay minerals and also weighted for the 6 most common non-clay minerals—quartz, k-feldspars, plagioclase, pyroxene, iron oxides, and glass (Table 2). The SC between average bedrock and seafloor samples in part reflects transport differences due to mineral density, mass, and shape (Syvitski and MacDonald, 1982). Thus, in analyzing Ross Sea sediment samples although it is a simple matter to distinguish volcanic rock from pre-volcanic basement, it is more difficult to distinguish Cenozoic alkaline volcanic rocks from Jurassic Ferrar dolerites, which doubtless have been transported by glacial erosion from the Transantarctic Mountains (TAM) into the Ross Sea (Fig. 3B). For this purpose, the presence of forsterite, as a surrogate for all olivines, has proven to be diagnostic.

Petrographic modal analyses of 19 MBL Cenozoic basaltic rocks (LeMasurier and Thomson, 1990) gave an average of 11.6% total olivine, with an average of 2.7% as phenocrysts. One sample was olivine-free, the others range from 5.0 to 21.6% total olivine. Phenocryst proportions for these samples range from 0–5.8%. Microprobe data on the compositions of these olivines indicate they are mainly in the range Fo85-90, with some zoned to rims of Fo50-70. By contrast, qXRD analysis of 14 Ferrar samples, provided by the U.S. Polar Rock Repository, yielded 0.0% (7 samples) to 0.7% forsterite (Suppl. Table S1), and 3.5%-10.9% quartz for the same samples. We have therefore assumed that all forsterite in Ross Sea cores was derived from the alkaline volcanic rocks of the West Antarctic rift.

Table 1
Location of the Ross Sea samples. List of the location of sites (Fig. 3A) and the qXRD weight % of the mineral compositions.

Cruise	Site		Long 0-360	Latitude	ENd (Farmer et al., 2006)	Quartz	K-feldspar	Plagioclase	Calcite	Dolomite	Siderite	Amphibole	Pyroxene	FeO	Forsterite	Amorphous silica	Kaolinite	Smectite	Illite	Biotite	Fe-Chlorite
NBP98-01	060-SMG	grab	181.78	−73.87		50.2	11.4	18.2	2.8	0.4	0.0	0.4	1.1	0.0	0.0	6.3	0.1	1.0	5.2	1.0	1.6
NBP98-01	061-SMG	grab	182.18	−73.81		48.8	10.9	19.6	1.9	0.3	0.0	0.6	0.7	0.0	0.0	8.1	0.0	1.8	5.7	1.1	0.6
NBP98-01	062-SMG	grab	182.44	−73.75		40.5	10.7	18.0	3.3	0.2	0.3	0.6	0.5	0.1	0.2	9.7	0.2	4.0	8.9	1.6	1.2
DF83	014-GB	grab	195.86	−78.48		16.6	6.6	10.9	0.0	0.0	0.0	0.0	0.0	0.0	0.0	22.9	3.3	14.6	20.2	2.7	2.0
DF83	019-GB	grab	201.30	−77.32		33.8	13.3	18.0	0.0	0.0	0.0	0.5	0.0	0.0	0.0	13.1	0.0	3.6	13.8	2.3	1.6
DF83	020-GB	grab	201.40	−76.89		53.5	15.3	18.4	0.0	0.1	0.0	0.4	0.6	0.0	0.0	6.1	0.0	0.7	4.2	0.8	0.0
DF83	021-GB	grab	201.96	−76.89		56.3	16.6	22.1	0.0	0.1	0.0	0.1	0.5	0.1	0.0	2.0	0.1	0.0	2.2	0.2	0.0
DF83	022-GB	grab	202.89	−76.88		23.0	7.2	14.5	0.0	0.0	0.0	0.0	0.0	0.0	0.0	0.1	0.7	6.5	37.4	3.8	6.4
DF83	023-GB	grab	203.39	−76.98		22.3	6.5	14.3	0.0	0.0	0.0	0.0	0.0	0.0	0.0	0.0	0.4	3.7	40.3	4.5	7.5
DF83	026-GB	grab	204.40	−76.95		23.1	7.9	14.5	0.0	0.1	0.0	0.1	0.0	0.0	0.0	1.1	0.2	5.0	35.1	4.0	9.0
DF83	025-GB	grab	204.49	−76.95		25.1	7.6	15.9	0.0	0.0	0.0	0.0	0.0	0.0	0.1	29.6	3.4	9.9	14.0	3.9	1.2
DF83	030-GB	grab	206.81	−76.60		32.6	5.0	14.0	0.8	0.0	0.0	0.1	0.0	0.0	0.0	0.5	0.0	3.0	33.0	3.1	8.0
DF83	029-GB	grab	207.35	−76.72		29.4	5.5	14.8	0.0	0.0	0.0	0.2	0.0	0.0	0.0	0.0	0.0	4.2	34.3	2.5	9.1
DF83	028-GB	grab	207.49	−76.83		28.9	6.1	15.2	0.0	0.0	0.0	0.1	0.0	0.0	0.0	1.0	0.0	3.1	33.9	3.3	8.2
ELT32	14		191.53	−75.00		21.4	9.4	14.4	0.0	0.7	0.5	0.4	2.0	0.2	0.8	7.0	1.4	11.1	4.9	0.3	7.0
ELT32	20		174.92	−77.58		17.4	7.7	13.3	0.0	0.4	0.3	0.0	0.3	0.1	0.3	30.7	0.3	7.5	7.5	3.2	0.0
ELT32	21		178.01	−77.93		14.7	5.4	11.2	0.0	0.2	0.4	0.1	0.0	0.2	0.4	40.0	0.8	9.8	11.7	4.0	1.5
ELT32	23		186.88	−78.38		22.7	10.6	14.6	0.0	0.2	0.7	0.4	0.0	0.2	0.0	24.1	1.9	7.8	10.5	3.9	2.7
ELT32	24		190.87	−78.40		16.6	8.0	11.9	0.0	0.1	0.6	0.0	0.2	0.5	0.2	37.9	1.4	7.1	9.3	2.5	0.4
ELT32	26		197.61	−78.07		16.6	8.0	11.9	0.0	0.1	0.6	0.0	0.2	0.5	0.2	38.2	1.4	7.6	10.9	3.3	0.6
ELT32	35		193.31	−77.05		30.7	10.6	12.8	0.0	0.2	0.4	0.1	0.9	0.3	0.0	15.5	1.9	9.2	11.9	3.2	2.1
ELT32	38		198.07	−76.98		28.5	10.2	13.5	0.0	0.1	0.4	0.4	0.2	0.2	0.0	14.7	2.7	6.3	16.3	2.9	3.8
	SAL298		196.62	−77.00		28.7	9.5	16.7	0.0	0.1	0.5	0.5	0.1	0.2	0.0	21.8	1.2	5.2	11.3	4.2	0.1
	SAL219		191.61	−82.22		29.5	10.2	17.2	0.0	0.1	0.4	0.5	0.0	0.1	0.0	18.4	1.2	5.2	11.7	4.4	1.2
ELT 32	12		183.10	−75.00		32.7	10.6	18.1	0.3	0.6	0.6	0.0	2.9	1.8	0.8	7.0	1.4	11.1	4.9	0.3	7.0
NBP94-01	22		171.68	−74.04		22.9	9.1	15.7	0.2	0.5	0.3	0.3	1.4	0.5	0.3	30.7	0.3	7.5	7.5	3.2	0.0
	39		187.74	−76.58	−5.77	25.2	8.7	18.4	0.0	0.1	0.3	0.3	0.8	0.3	0.0	22.5	1.5	6.0	10.4	4.2	1.2
	22		171.68	−74.04		22.9	9.1	15.7	0.2	0.5	0.3	0.3	1.4	0.5	0.3	30.7	0.3	7.5	7.5	3.2	0.0
	33		180.38	−75.46		20.3	6.6	13.6	0.0	0.2	0.5	0.0	0.0	0.2	0.2	37.9	1.4	7.1	9.3	2.5	0.4
	32		179.39	−75.46		16.8	7.0	12.8	0.0	0.3	0.4	0.0	0.4	0.1	0.2	38.2	1.4	7.6	10.9	3.3	0.6
NBP95-01	12		177.82	−76.78	−9.62	25.2	8.4	15.3	0.4	0.3	0.5	0.3	0.9	0.2	0.0	25.0	1.5	5.3	12.1	4.6	0.0
	9		182.06	−76.04		21.2	8.7	14.4	0.4	0.5	1.1	0.3	0.0	1.7	0.4	23.5	1.0	11.9	10.8	3.0	1.2
	11		180.91	−76.45	−10.10	21.2	8.7	14.4	0.4	0.5	1.1	0.3	0.0	1.7	0.4	23.5	1.0	11.9	10.8	3.0	1.2
	21		185.62	−76.19		24.9	9.4	15.1	0.1	0.4	0.7	0.3	0.6	0.2	0.4	25.8	1.1	4.4	11.6	4.0	1.0
	18		179.54	−77.33		21.1	10.1	13.5	0.0	0.0	0.5	0.0	0.0	0.1	0.3	27.8	2.5	6.2	12.5	3.8	1.7
	6		180.64	−75.50		22.9	9.1	15.7	0.2	0.5	0.3	0.3	1.4	0.5	0.3	30.7	0.3	7.5	7.5	3.2	0.0
	24		184.58	−76.61	−8.08	25.0	9.2	17.2	0.0	0.0	0.4	0.3	1.1	0.2	0.0	20.1	1.2	7.5	13.0	3.4	1.3
	17		179.05	−77.45	−12.50	24.8	6.2	12.5	0.6	0.4	0.5	0.4	1.0	0.7	0.3	36.8	0.0	5.5	7.1	3.2	0.0
DF80	193		165.02	−76.55		21.3	10.4	18.7	0.0	0.0	0.4	0.2	3.3	0.4	0.4	25.8	0.0	9.6	5.9	3.3	0.3
	109		166.72	−75.07		18.5	7.8	12.9	0.0	0.3	0.2	0.0	1.1	0.3	0.0	40.9	1.6	7.8	5.5	2.8	0.3
	112		166.82	−74.92	−3.76	19.6	7.5	12.3	0.0	0.2	0.4	0.0	0.0	0.2	0.8	45.0	0.8	8.5	6.1	2.1	0.6
	57		166.82	−77.28		3.4	8.2	14.8	0.2	0.2	0.8	0.8	4.8	2.3	0.8	45.0	0.8	8.5	6.1	2.1	0.6
	99		165.27	−75.52		19.6	8.3	16.1	0.0	0.0	0.2	0.3	3.2	0.5	0.1	36.2	0.0	3.2	8.1	2.8	1.6
DR87	30		170.85	−73.20		26.4	12.9	17.4	0.0	0.1	0.9	0.3	2.3	0.4	0.1	15.4	0.4	9.6	10.3	2.3	1.4
	32		170.39	−73.48		3.5	10.1	14.0	0.3	0.5	0.9	0.8	2.6	0.5	1.6	47.3	1.0	0.9	9.5	3.8	2.8
ELT32	13TW					16.0	10.1	13.2	0.0	0.4	1.1	0.7	0.0	0.3	0.9	25.7	2.5	8.8	13.9	3.3	3.1
DR87	30		170.85	−73.20		26.4	12.9	17.4	0.0	0.1	0.9	0.3	2.3	0.4	0.1	15.4	0.4	9.6	10.3	2.3	1.4
	32		170.39	−73.48		3.5	10.1	14.0	0.3	0.5	0.9	0.8	2.6	0.5	1.6	47.3	1.0	0.9	9.5	3.8	2.8

Table 2
Mineral averages and standard deviations. Average qXRD weight % estimates for samples of basalt (B), dolerite (D), hyaloclastite (H), gneiss (Gn), and granite (Gr) from West Antarctic and for the Ross Sea (RS) and East Greenland (EG) marine sediment samples, and Similarity Coefficients for 15 non-clay and clay minerals (above the diagonal) and weighted 6 major non-clay minerals below the diagonal.

	E Grn'lnd		Ross Sea		Basalt		Hyaloclastites		Dolerite		Gniess		Granite	
	Average	stdev	Average	stdev	Average	stdev	Average	stdev	Average	stdev	Average	stdev	Average	stdev
Quartz	3.7	0.64	23.7	10.18	0.3	0.26	0.34	0.50	5.8	3.52	19.9	21.25	28.8	5.80
KSPAR	4.1	4.14	8.5	2.57	4.8	2.34	0.98	0.72	6.2	2.50	3.2	1.59	21.0	15.06
Plag	31.9	1.61	14.7	4.04	34.3	7.24	29.87	7.29	33.2	10.57	37.6	17.26	38.5	12.18
Calcite	0.1	0.10	1.0	4.82	1.7	2.40	2.06	0.58	0.7	0.35	0.2	0.36	0.1	0.26
Dolomite	0.0	0.04	0.7	2.71	0.0	0.11	0.26	0.42	1.1	0.76	0.3	0.52	0.2	0.22
Siderite	0.0	0.03	0.4	0.34	1.9	0.56	1.81	0.70	0.6	0.31	0.2	0.36	0.0	0.00
Amphibole	0.4	0.38	0.3	0.31	2.0	0.91	2.15	0.50	0.7	0.49	13.5	14.87	1.4	1.11
pyroxene	17.2	1.51	1.4	2.81	18.9	4.99	11.02	5.80	13.7	6.09	4.2	8.30	0.5	0.67
FeO	4.4	0.63	0.6	1.07	4.5	1.85	3.93	2.25	5.1	2.15	0.7	0.93	0.1	0.15
Forsterite	0.3	0.23	0.3	0.50	9.1	3.38	7.39	1.69	1.0	0.69	1.2	2.20	0.0	0.11
Volcanic glass	8.9	2.12	23.7	12.91	9.5	1.05	18.82	4.22	13.4	10.58	1.9	2.35	2.0	1.07
Kaolinite	0.3	0.56	1.4	1.87	0.1	0.25	0.0	0.0	1.5	4.36	0.1	0.17	0.2	0.44
Smectite	15.8	1.63	6.5	3.05	5.4	2.09	14.16	4.64	10.9	5.66	4.1	4.53	0.3	0.51
Illite	6.0	0.96	11.8	8.70	6.2	2.56	0.01	0.02	4.0	2.60	2.4	3.23	2.4	1.24
Biotite (2M1)	1.5	0.47	3.0	1.11	0.1	0.28	2.24	0.81	0.8	1.15	8.8	5.05	4.3	4.28
Fe-Chlorite (Tusc)	5.4	1.10	1.9	2.37	1.2	1.37	1.52	1.39	1.2	2.13	1.7	2.87	0.2	0.25

Similarity Coefficient
$n = 15$

$n = 5$	EG	RS	B	H	D	GN	GR
EG	100.0	33.80	44.2	33.90	49.7	27.90	24.90
RS	33.8	100.0	29.9	31.20	48.3	39	26.06
B	78.2	26.64	100.0	54.10	40.0	30.29	21.86
H	54.6	28.14	63.2	100.00	33.8	22.23	16.17
D	76.2	36.59	68.1	56.67	100.0	25.92	19.77
GN	40.6	46.59	36.4	26.69	38.0	100.00	36.11
GR	38.0	39.04	23.4	17.12	26.3	51.60	100.00

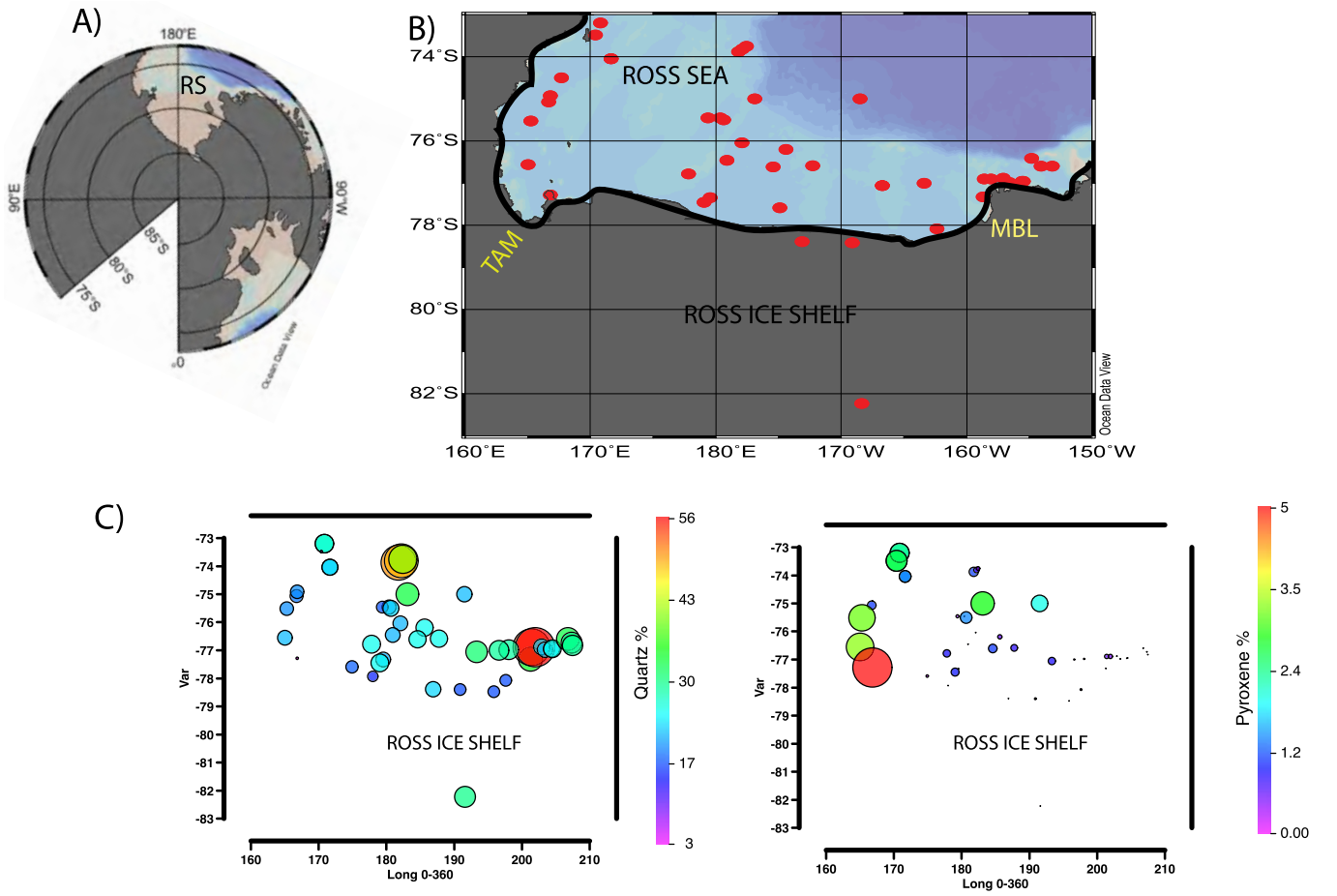

Fig. 3. A) Map of Antarctica showing the Ross Sea (RS); B) Location of surface and core samples (Table 1; Fig. 1). TAM = TransAntarctic Mountains; MBL = Marie Byrd Land. C) Bubble plots of the weight % of quartz and pyroxene in the surface/near surface samples. (For interpretation of the colors in the figure(s), the reader is referred to the web version of this article.)

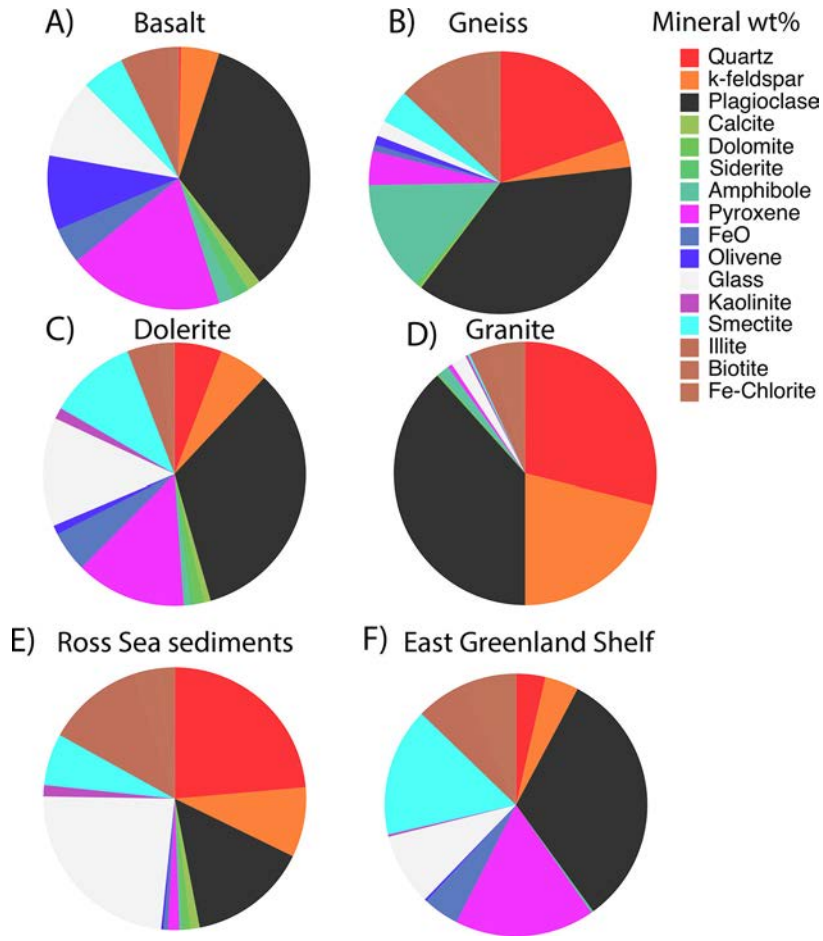

Fig. 4. Pie diagrams of the average mineral composition of four bedrock types (A, B, C, and D) from West Antarctic and glacial marine sediments from the Ross Sea (E) and East Greenland Shelf.

The presence of phenocryst olivine in these rocks is important. Subglacial eruptions yield pillow lavas and hyaloclastites with a high proportion of glass (Fig. 2). Olivine that occurs as groundmass olivine in subaerial lavas would be less likely to be found in their subglacial equivalents, whereas phenocrysts of olivine would invariably be found in these deposits because they were present in the magma prior to eruption.

As part of our study we also processed 7 basalt, 5 gneiss, 6 samples of granite, and 5 hyaloclastites from rock or powdered samples of West Antarctic bedrock that we (WEL) had on hand or were obtained courtesy of the Core Repository at Ohio State University. In order to provide comparative data to the Ross Sea sediments these samples were processed for their mineral wt% using the Rockjock v6 whole pattern approach (Table 2; Suppl. Table 1). We compare the mineral composition of the Ross Sea sediments with those we have previously reported from off the East Greenland 60,000 km^2 heavily glacierized outcrop of early Tertiary flood basalts (Andrews et al., 2015; Brooks and Nielsen, 1982; Larsen, 1983) (Fig. 4), and which overlies Archaean and Paleoproterozoic granites and gneiss. As an example, MD99-2317 lies ~50 km off the East Greenland coast and contains a detailed record of late glacial and Holocene change (Jennings et al., 2011).

3.2. Previous provenance studies

Golledge et al. (2013, their Fig. 13) show projected ice flow trajectories and transport paths "....inferred from sediment outcrops and core data (Licht et al., 2005)." Indeed considerable work on sediment provenance has been previously reported (reviewed by Licht and Hemming (Licht and Hemming, 2017)). The methods range from sand petrology, radiogenic isotopes, and geochemical fingerprinting (Pereira et al., 2018). The main focus in these studies has been on the identification of the sediment signatures of various ice streams with the goal of reconstructing past changes in glaciological regimes (Farmer and Licht, 2016; Farmer et al., 2006; Palmer et al., 2012; Pereira et al., 2018). Farmer et al. (2006) presented a comprehensive geochemical study on basal till samples from 10 cores from the Western, Central, and Eastern Ross Sea from samples collected previously (Licht, 1999). We also processed samples from these cores (Table 1). Thus, there has been considerable effort to determine the ages of bedrock beneath the WAIS but non-clay and clay mineral qXRD compositions have not been extensively applied to provenance studies, although as noted earlier, studies of clay-size mineralogy have been reported from the Amundsen embayment (Ehrmann et al., 2011).

4. Results and a test of the hypothesis

We processed 76 sediment samples (including repeated analyses) from 48 sites (Table 1, Suppl. Table 1, Fig. 3A) collected during a number of research cruises. Recent evidence indicates that many of these sites would have been exposed during a late Holocene collapse of the Ross Ice Shelf (Yokoyama et al., 2016). The prevailing ocean surface transport is from east to west (Dotto et al., 2018), which could result in some sediment transport and mixing. We focused on surface and near-surface samples. The transect extends for approximately 1400 km between 160° and 210° longitude (Fig. 3A). INSTAAR sediment reserves (GRL#) were used from pre-

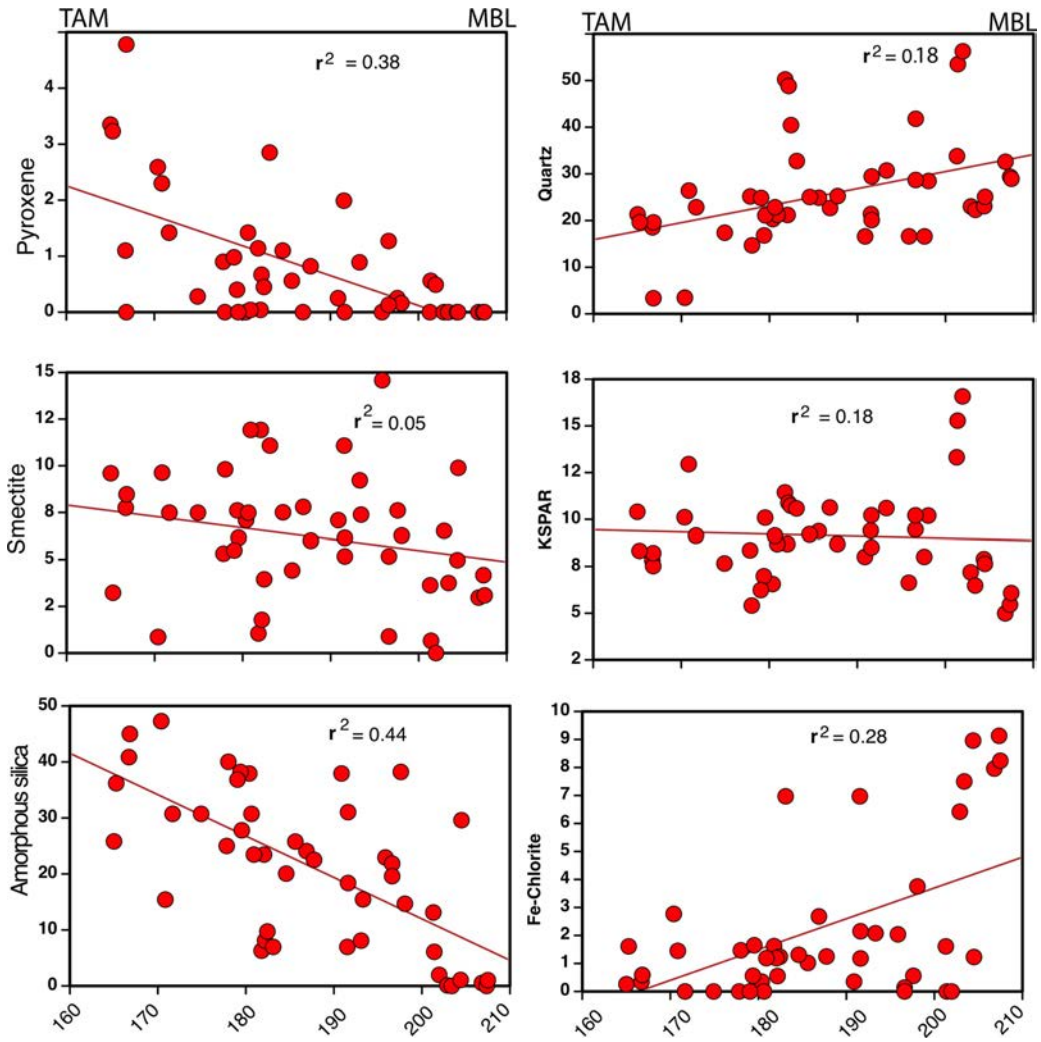

Fig. 5. Biplots of the distribution of mineral weight %s versus west (TAM = TransAntarctic Mountains) to east (MBL = Marie Byrd Land (see Fig. 1)) longitude of Ross Sea samples and the significance (r^2) of the trend. A) pyroxene, B) smectite, C) amorphous silica, D) quartz, E) K-spar, F) Fe-chlorite.

vious studies (Licht, 1999) and additional samples were obtained from the sediment archives curated at Oregon State University. A few of the samples contained clasts >2 mm and although no grain-size measurements were taken the majority of the samples are mud, i.e. <63 μm in grain-size. The total includes 51 samples from individual sampled sites, including two samples from beneath the Ross Ice Shelf that were also studied in the Farmer et al. (2006) study (Fig. 3A, Table 1), plus samples from various depths in some cores and replicate samples, (Suppl. Table 1).

Pie diagram plots of the spatial and average distribution of the mineral wt percentages of 49 sites (Fig. 4E) show the dominance of quartz and feldspars in the assemblages, but with a significant fraction of amorphous silica, which includes volcanic glass from hyaloclastites, pillow lavas, diatoms, and the products of overgrinding the sediments (from glacial abrasion and the qXRD milling procedure (Andrews et al., 2013). Characteristic minerals for the presence of eroded basalt bedrock, such as forsterite and pyroxene occur in low wt percent (Figs. 4E and 5A; Table 2) and smectite is relatively abundant with a maximum estimated wt percent of 15% (Table 2, Fig. 5B). It can be an indication of weathering of basalt. However, given the long glacial coverage of Antarctica it is unlikely that any postulated subglacial volcanic rocks have a cover of chemically altered bedrock. Smectite can, however, indicate chemical weathering on a variety of bedrock as is evident by its presence in glacial marine sediments from around the Labrador Sea and Baffin Bay (Andrews et al., 2020; Boyd and Piper, 1976; Piper and Slatt, 1977) derived from erosion of Tertiary shelf and basin accumulations. It is difficult to compare the 20–30% estimates of smectite in the Amundsen embayment (Ehrmann et al., 2011) with our data (Fig. 5B) because of the differences in methodology (see earlier), although the weight percent of smectite tends to decline eastward toward Marie Byrd Land (Fig. 5B) as does amorphous silica (Fig. 5C). The plots of the weight percent of quartz and k-feldspar have either a weak trend to increase to the east or no trend.

The mineral composition of the sediment samples is radically different from either the alkali basalts and hyaloclastites, or the Ferrar dolerite and the Ross Sea sediments are much closer in composition to the gneiss and granite bedrock compositions. This is also evident in the tri-plots of minerals from both the bedrock and sediment samples (Fig. 6). There is also a significant contrast between the composition of the samples from the Ross Sea compared to those from off East Greenland (Fig. 4E versus F, Table 2). The East Greenland samples clearly record a dominant basalt source (Andrews et al., 2015) with large percentages of plagioclase and pyroxene, and small amounts of quartz and K-feldspar (Table 2).

Erosion of subglacially erupted volcanic rocks (Fig. 2) from beneath the WAIS should result in measurable quantities of volcanic glass, analcime and chabazite. Estimates of their zeolite wt%s were obtained by processing the Rjv6 intensity data in the zincite version of the USGS Rjv11. Only 7 sites had wt percentages of

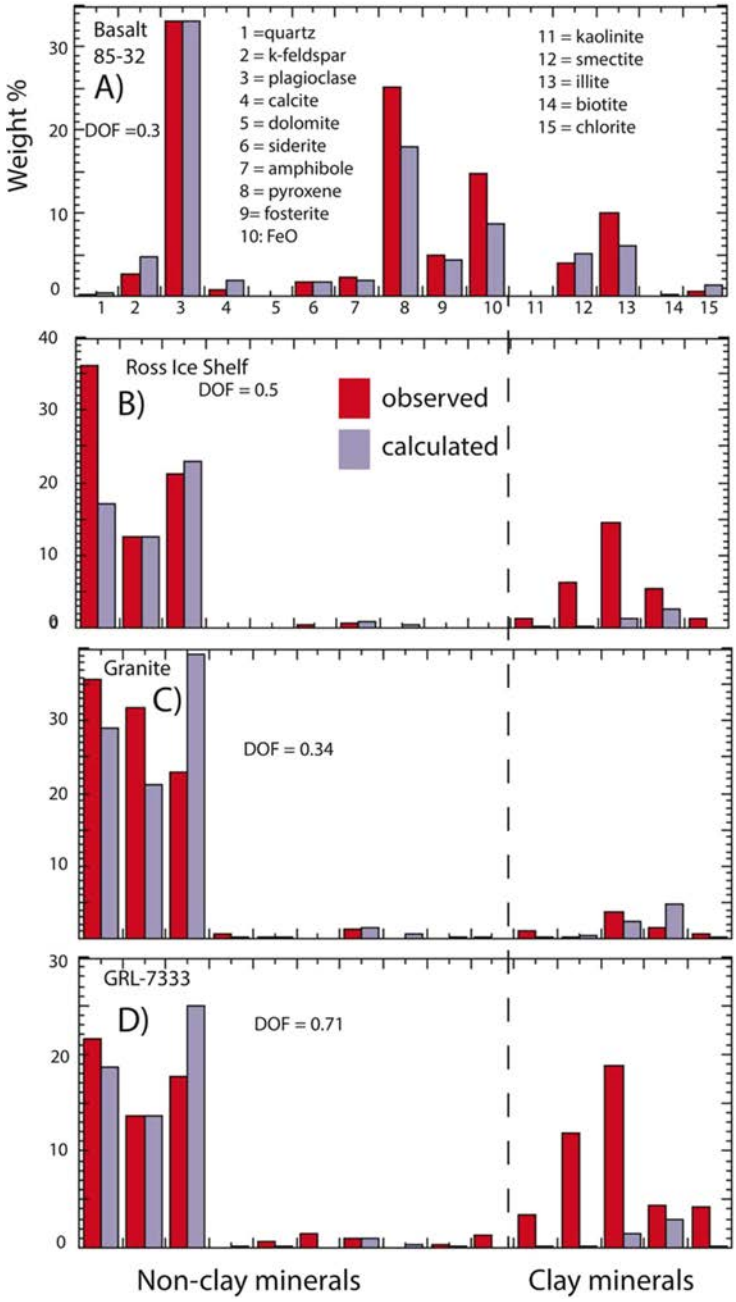

Fig. 6. Relative weight % (the three minerals are forced to sum to 100%) of the bedrock mineral composition and compared with the composition of glacial marine sediments from the Ross Sea and off the East Greenland basalt outcrop (MD99-2317).

chabazite >3% and only one site had analcime wt% >2%. The samples from these sites contained little or no pyroxene but they were located along the western boundary of the Ross Sea, and thus close to the TAMs and extension of the East Antarctic Ice Sheet into the Ross Sea.

5. Discussion

The results of the qXRD results need to be evaluated in the light of the glacial and marine sediment pathways. The glacial sediment pathway is strongly influenced by the basal temperature (Licht and Hemming, 2017; Hooke et al., 2013), which controls whether the sediments produced by plucking and abrasion at the glacial/bedrock interface (Boulton, 1996; Stokes, 2018) remains in the traction zone or becomes englacial (Hooke et al., 2013). Clark (1987) showed that in sediment transported subglacially the composition was diluted by 50% over distances of 30 to 60 km, whereas englacial transport can be much greater (Prest, 1990). The release of coarse-grained sediment at the grounding line of the ice area/ice shelf system indicates that the under-shelf sediments would be fine-grained and generally lack IRD (McKay et al., 2016; Alley et al., 1989; Anderson and Bartek, 1991; Bartek and Anderson, 1991).

Fig. 8A summarizes our conceptual model. The bedrock at the base of the WAIS could potentially consist of granitoid or basaltic facies and the ? mark in this figure highlights the question we address. At the two sites under the Ross Ice Shelf the mineral assemblages are clearly felsic in origins (Fig. 8A and B), although the wt% of smectite and glass differ from the granitoid bedrock. The similarity coefficient indicates a close association between the sed-

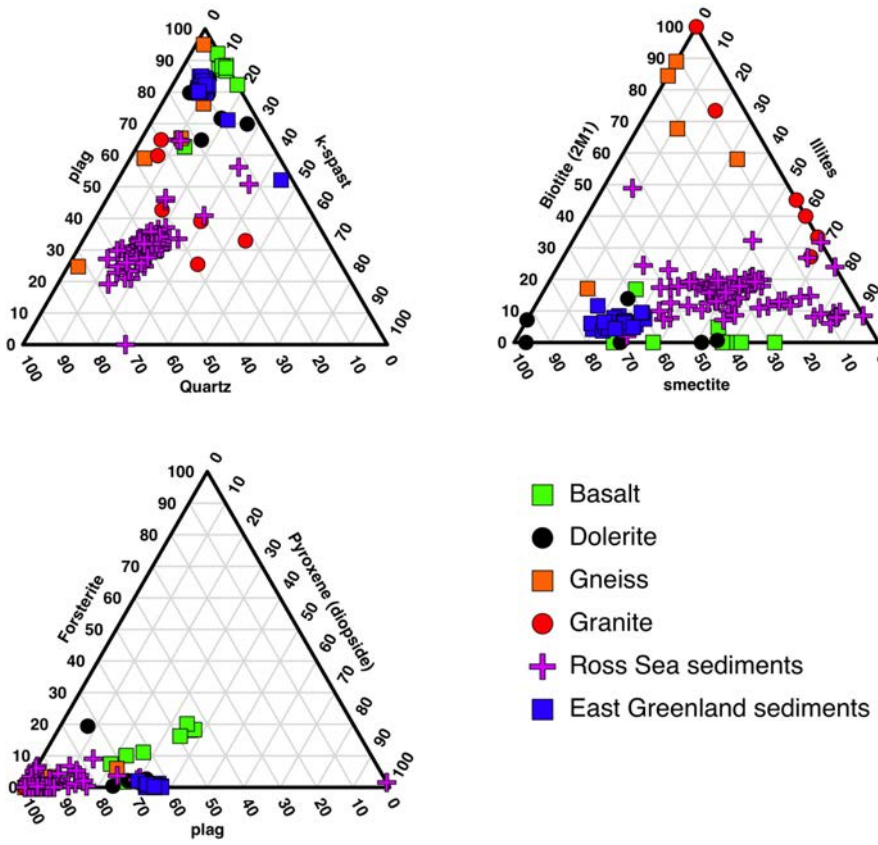

Fig. 7. Showing the results of the SedUnMix program with four bedrock sources (basalt, dolerite, gneiss, and granite). Observed (red) versus calculated (blue) percentages for A) basalt bedrock sample, C) a granite bedrock sample, B) and D) for samples from the Ross Ice Shelf and Ross Sea (Table 1; Suppl. Tables 1 and 2) (GRL-7333 is from core ELT32 13TWC, Table S1). The degree-of-fit (DOF) for these specific samples are also listed.

iments under the Ross Ice Shelf and those recovered from the Ross Sea (SC $>$ 0.6). The ocean circulation under the ice shelf (Smethie and Jacobs, 2005) would entrain meltwater plumes and transport the suspended sediment toward the shelf front and the Ross Sea (Fig. 8A), but the similarity between the Ross Sea and Ross Ice Shelf compositions could imply bottom current transport under the ice shelf. The large percentages of glass in Ross Ice Shelf samples might reflect deposition from tephras deposited on the ice sheet (Iverson et al., 2017).

The results of the SedUnMix analyses indicate that the samples from the Ross Sea have a close link to the West Antarctic granite bedrock samples and have only limited association with mafic bedrock (Suppl. Table 2). These results indicated that the five bedrocks, alkali basalt (and hyaloclastites), dolerite, gneiss, and granite are reasonably well predicted (Fig. 7) with average correct classifications respectively of 80%, 63%, 63%, and 74% and little overlap between the two volcanic versus the igneous/metamorphic bedrocks. The Degree of Fit (DOF) for the bedrock samples varied from 0.16 to 0.59 and for the sediment samples on average significantly higher 0.41 to 0.78. The plots of observed versus calculated mineral wt% (Fig. 6) indicated that the largest differences in the Ross Sea sediments were in the over-estimation of quartz (Fig. 6B and 6C) and under-estimation of the wt% clay minerals and this is the primary explanation for the "unaccountable fraction" being relatively large (~40 $\pm$ %) (Suppl. Table 2). These results, plus the SC values between bedrock and seafloor samples (Table 2), indicate that during glacial erosion and subsequent meltwater transport the bedrock compositional signatures are modified (Andrews, 1987; Syvitski and MacDonald, 1982).

The sediment unmixing model indicates that there is no appreciable change in the estimated percentage of granite between the western, central, and eastern Ross Sea (Fig. 8B), and the two samples from beneath the RIS (Fig. 8A and B) are estimated to be composed of between 56 and 61% granite with the compositions being significantly enriched in quartz and illite. The compositions of the Ross Sea sediments (Figs. 3B and 5) show a strong affinity with the granite bedrock but with an inclusion of dolerite in some sites, particularly in the Western Ross Sea (Suppl. Table 2). Only two samples have any marked alkali basalt affinity. On the Geological Map of Antarctica (Craddock, 1972) it can be seen that there are only two major exposures of Cenozoic volcanic rock in the area of the western Ross Sea shown in Fig. 3B, one at Franklin Island and the other on Ross Island (Fig. 1). These localities account for the two occurrences of high pyroxene in western Ross Sea cores shown in Fig. 3C. The onshore bedrock exposures between these two localities consist of (1) Cambrian – Ordovician granitic rocks of the Granite Harbor Intrusives, (2) Devonian – Jurassic Beacon Group sandstones which include tabular mafic Ferrar Intrusives, and (3) the Jurassic Ferrar basaltic volcanic rocks located inland of Ross Island. Ferrar basaltic rocks, intrusive and extrusive, are represented by the "dolerite" of this study. This bedrock suite easily accounts for the quartz and pyroxene wt%s in western Ross Sea cores (Fig. 3C). The two samples collected from under the Ross Ice Shelf (Sal219 and Sal 298, Table 1) both have high quartz wt%s and limited contributions from the other bedrock types.

However, the results also indicate that a significant fraction was not assigned to any of the bedrock end members, averaging 41 $\pm$ 10%, Inspection of the individual mineral residuals (Suppl. Table 3) indicates that the size of the residuals was dominated by large excursions in quartz and illite indicating that, relative to the source bedrock, the Ross Sea sediments are enriched in these minerals. However, it is obvious that the assemblages from the Ross Sea and under the Ross Ice Shelf are primarily associated with a granite-like mineral composition with only a limited number of

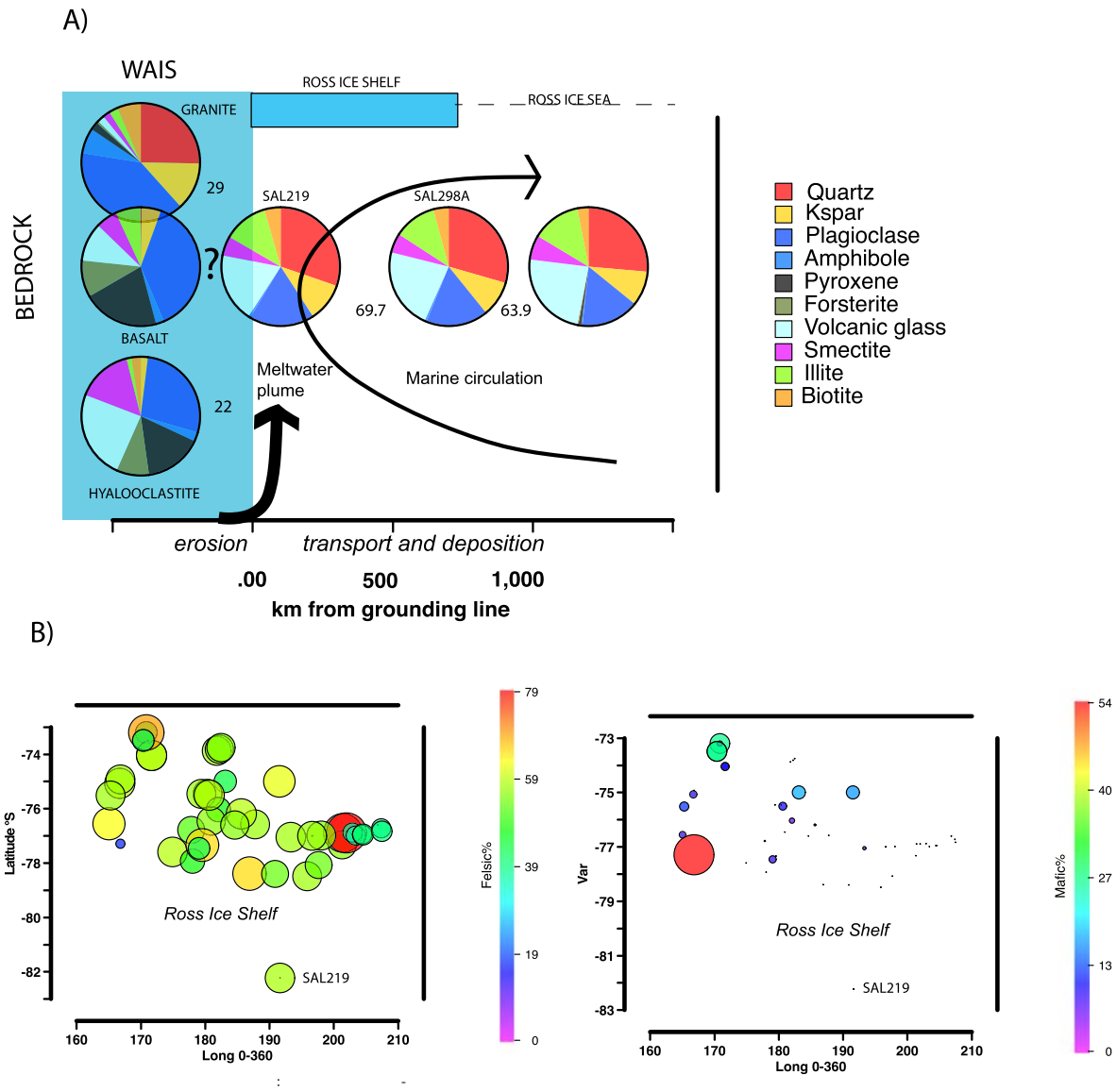

Fig. 8. A) Schematic cross-section through the Ross Ice Shelf ca 160°(see Fig. 3) to the Ross Sea. Possible mineral compositions are shown in pie diagrams for three bedrock types and for sediments retrieved from under the ice shelf and the average composition of Ross Sea sediments. Circulation under the shelf is shown (Smethie and Jacobs, 2005). Similarity coefficients (e.g. 69.7) are shown for adjacent samples. B) Results of the SedUnMix analysis for the Ross Sea sediments are shown for percent estimates of felsic and mafic end members.

Table 3
Correlations (Pearson's r) between longitude of the samples (Figs. 3A and 5; Table 1) and mineral weight %.

Mineral	Pearson's	Mineral	Pearson's
Quartz	0.42	K-feldpar	−0.06
Plagioclase	0.07	Dolomite	−0.62
Kaolinite	0.08	Calcite	−0.42
Illite	0.60	Amphibole	−0.49
Biotite	0.01	Pyroxene	−0.67
Chlorite	0.53	FeO	−0.42
Fosterite	−0.49		
Amorphous silica	−0.67		
Smectite	−0.23		

sites offshore from the TAM showing any influence of alkali basalt in their compositions (Fig. 3).

Some volcanic debris might have been expected to be delivered to the rift interior from exposed volcanoes of the MBL province that are not on the seaward side of the WAIS divide (Fig. 1), e.g. the Executive Committee Range (ECR). However, these are the highest elevation volcanoes in the province, and are unlikely to have experienced significant erosion from the cold-based ice sheet since 15 Ma at the latest. Furthermore, no significant amounts of hyaloclastite are exposed in these volcanoes. Finally, it is not clear whether the ice sheet drains northward or southward from its high point in the ECR. It seems clear that several factors can easily explain the lack of detritus from MBL volcanoes in the WAIS.

An argument might be made that a more volcanic signature might be apparent in sediments dating from LGM deglaciation. We only processed four samples from cores where we had sediments from both the surface and farther downcore (Suppl. Table 1) and we note that obtaining any accurate age estimate in this region is extremely difficult (Andrews et al., 1999, 1997). However, more recent coring efforts in the Whale Deep Basin have obtained radiocarbon dates on foraminifera. The average bias between the estimated wt% of the surface and downcore sediments is small with values between 0.7 and 4.1% with little or no forsterite or pyroxene (Table 4). This is admittedly a very small sample, but the geographic coverage of the sites (Table 1) gives us some confidence

Table 4
Surface versus downcore mineral wt%s and the bias (absolute difference) between them and the average bias.

Core site	Quartz	k-spar	plag	Calcite	Dolomite	Siderite	Amphibole	Pyroxene	FeO	Forsterite	Amorphous silica	Kaolinite	Smectite	Illites	Biotite	Fe-Chlorite	Average bias (%)
20PC 1.5	17.4	7.7	13.3	0.0	0.4	0.3	0.0	0.3	0.1	0.1	38.5	1.2	8.3	9.6	2.6	0.0	
20PC 170	16.4	6.1	11.6	0.0	0.5	0.5	0.0	0.0	0.2	0.7	42.9	3.0	10.0	6.3	1.8	0.0	
bias	1.0	1.5	1.8	0.0	0.1	0.2	0.0	0.3	0.2	0.6	4.4	1.8	1.7	3.3	0.7	0.0	1.1
24PC 6	16.6	8.0	11.9	0.0	0.1	0.6	0.0	0.2	0.5	0.1	29.6	3.4	9.9	14.0	3.9	1.2	
24PC 429	27.1	9.5	15.6	0.0	0.2	0.5	0.4	0.2	0.2	0.0	23.4	1.4	4.8	11.1	3.8	1.9	
bias	10.5	1.5	3.7	0.0	0.2	0.1	0.4	0.1	0.2	0.1	6.2	2.0	5.1	2.9	0.1	0.7	2.1
35PC 1	30.7	10.6	12.8	0.0	0.2	0.4	0.1	0.9	0.3	0.0	15.5	1.9	9.2	11.9	3.2	2.1	
35PC 264	31.8	10.2	11.1	0.4	0.6	0.4	0.9	0.0	0.3	0.0	14.1	1.9	9.0	14.4	2.2	2.0	
bias	1.1	0.4	1.7	0.4	0.4	0.0	0.8	0.9	0.0	0.0	1.3	0.1	0.2	2.5	1.0	0.0	0.7
26G	23.1	7.9	14.5	0.0	0.1	0.0	0.1	0.0	0.0	0.0	1.1	0.2	5.0	35.1	4.0	9.0	
26PC 246	28.5	11.0	13.1	0.3	0.2	0.8	0.2	1.0	1.0	0.0	19.8	1.5	6.2	11.2	3.8	1.7	
bias	5.4	3.1	1.5	0.3	0.1	0.8	0.1	1.0	1.0	0.0	18.7	1.3	1.3	23.8	0.2	7.2	4.1

to conclude that there is probably no significant evidence for erosion of volcanic bedrock over the last deglacial period.

The possibility that a large volume of young volcanic rock lies beneath the WAIS has severe implications for global sea level change, because of the possibility of renewal of this activity. It has been said that the greatest uncertainty in future sea level rise is the rate of melting of the West Antarctic and Greenland ice sheets (Church et al., 2013; Bamber et al., 2019; Kopp et al., 2019), which would certainly be exacerbated by large-scale subglacial volcanic eruptions in West Antarctica and have global repercussions. The results of our study suggest this is not a likely scenario. Nevertheless, the uncertainties inherent in this study require a careful evaluation of all sides of this debate.

Our study of the mineral composition of sediments from the Ross Sea and ice shelf does not provide any estimate of the ages of the source bedrock, although that was provided for some of our core sites by the study of Farmer and colleagues (Farmer and Licht, 2016; Farmer et al., 2006) (Table 1). Farmer and Licht (2016) report the results of a Nd, Sr, and Pb isotopic study of 14 onshore and 21 offshore tills in the Ross Sea area, covering much of the area of our study. Their data cluster in the isotopic space occupied by data for the Admiralty Intrusive Suite, Ferrar mafic rocks, and other pre-Cretaceous rocks of the TAM on the western Ross Sea coast, with one exception. The single sample with Nd, Sr, Pb isotopic values like those of the late Cenozoic alkali basalts lies ~65 km south of Ross Island, within one of the largest occurrences of late Cenozoic volcanic rocks in the western Ross Sea (Craddock, 1972). Farmer and Licht note the "unexpected — lack of major involvement of Late Cenozoic volcanic rocks as source of glacial till in West Antarctica." They conclude that these rock types were not eroded from beneath the major ice streams that drain the WARS. These results are much like those that we report here, but from a completely different data set, which strongly supports our conclusions. Our data (Figs. 3C and 5) confirm the importance of glacial transport of Ferrar mafic volcanic-derived sediment across the TAM and the weight % of pyroxene declines steadily eastward across the Ross Sea (Fig. 5A). There is no sign of a seaward "bulge" in the weight % of pyroxene, which would be expected if late Cenozoic alkaline basalts floored a large fraction of the subglacial bedrock of the WARS. It is also noteworthy that the percentages of these minerals decrease eastwards toward MBL (Fig. 5). These conclusions are also supported by the modeling of the Antarctica Ice Sheet during the LGM (Golledge et al., 2013). However, the validation of glacial erosional models require sediment volumes, sediment density, and a chronology from adjacent lake or ocean depositional basins (e.g. Bell and Laine, 1985; Hallet et al., 1996) and as yet this has not been attempted for the Ross Sea.

In our approach, sediment mixing and changes in provenance are seen in the persistent decrease of percentages of glass toward MBL and the eastern Ross Sea (Fig. 7C; Table 3), as well as in the estimated isolated presence of pyroxene in samples from the western Ross Sea compared to samples from the central or eastern Ross Sea (Fig. 3C). Other minerals which indicate a statistically significant increase or decrease across the Ross Sea ($p < 0.05$, $r = 0.275$; Table 3) can be grouped into felsic non-clay and clay minerals which show an increase (e.g. quartz, illite, chlorite) versus those linked to alkali basalt and dolerite (pyroxene, forsterite, and smectite) which decrease from west to the east (Fig. 5A and C).

In six instances we have paired qXRD data and isotopic data (Farmer et al., 2006). These samples show no evidence for an alkali basalt derived mineralogy and their compositions are predicted to have been derived from granite bedrock. However, our samples (Table 1) are primarily from grab and core tops, and the limited comparison that we can make with down-core sediments did not reveal any obvious change in mineral composition. We note that our results are consistent with those of Vogel et al. (2006).

They acquired subglacial sediment samples from 5 localities across the rift interior, from which they collected >500 pebbles. Among these, only two basalt pebbles were found. They were from only one of the five localities (Byrd Station) and they were determined to be Mesozoic to Cambrian in age. The rest of the >500 pebbles were granites and gneisses. Vogel et al. (2006), offer two options to explain the disparity between their results and those of Behrendt et al. (1993): (1) The proposed large igneous province does not exist, and previously reported subglacial activity was limited to individual centers such as those described by Blankenship et al. (1993). (2) Other highly magnetic, non-Cenozoic rocks are responsible for the observed magnetic anomalies. They provided several examples of the latter explanation, including ones where they measured magnetic susceptibilities of several appropriate rocks from the Polar Rock Repository at Ohio State University.

Van Wyk De Vries et al. (2017) identified 138 subglacial "conical edifices" distributed mainly along the axial trough of the WARS, based on morphometric analysis and the coincidence of the cones with circular magnetic anomalies. Most lie in the Ross Sea drainage, but many lie on the east side of the WAIS divide where they could not have contributed detritus to our area of study. They assigned a "confidence factor" to each cone based on the degree to which it was associated with concentric magnetic and/or gravity anomalies. They infer that many of these may be Pleistocene or younger in age, based on the undissected nature of the cones. Though they cite Vogel et al. (2006), they do not acknowledge their findings nor address the problem those findings present.

Neither Behrendt et al. (1993) nor Van Wyk De Vries et al. (2017) have considered the fact that the large volumes of subglacial volcanic rock they have proposed should be represented by correspondingly large volumes of glass-rich hyaloclastites and pillow lavas, like those found at the base of many exposed volcanic sections across the MBL dome. These deposits are easily eroded and disaggregated, even in the typically non-erosive polar glacial environment (LeMasurier and Rocchi, 2005; Rocchi et al., 2006). Erosion of pillow lavas would yield more glass-rich clasts than subaerial lavas.

It follows that, if there is indeed a large volume of subglacial volcanic rock in the WARS, we should expect to see significant amounts of glass, of zeolites (phillipsite, chabazite, analcime) and of smectite, as well as olivine carried to the surface as intratelluric crystals, which would appear as phenocrysts in subaerial lavas and pillow lavas. As noted earlier the results of our analyses (Figs. 3 and 8C) show an increase of volcanic glass *westward*, and even evidence for alkali basalt at two sites on the extreme western limit of the Ross Sea, both of which are the reverse of what would be expected if large volumes of volcanic rock were concealed beneath the WAIS.

Several other geological and geophysical observations provide information relevant to the possibility that a large volume of late Cenozoic volcanic rock exists beneath the WAIS in the interior of the WARS. Winberry and Anandakrishnan (2004) used data from the Antarctic Network of Unattended Broadband Seismometers (ANUBIS) and from the Global Seismic Network station at the South Pole to interpret characteristics of the lithosphere along a transect that extends across the MBL dome and rift interior to the Transantarctic Mountains. Their results suggest that the rift interior is underlain by "normal mantle" and is not volcanically active at present. They note that this is consistent with the finding of faster mantle velocities in the rift interior compared with those beneath the MBL dome (Ritzwoller et al., 2001). Lloyd et al. (2015) came to similar conclusions based on results obtained from a denser transect across West Antarctica. Winberry and Anandakrishnan (2004) acknowledge that this interpretation conflicts with Behrendt et al. (1993) and suggest that the magnetic anomalies they cite may be relict features from an earlier period of extension.

LeMasurier (2008) compared the bedrock elevation of the WARS with rifts of similar scale and crustal thickness, by calculating the mass equivalent of glacial ice as in unconsolidated sediment at 7 localities, and then recalculating bedrock elevations. The results show that the rift floor of the WARS lies 1000-2000 m lower than the Basin and Range province, the Rio Grande rift, and the East African rift, suggesting the interior of the WARS is relatively cool and volcanically inactive, consistent with the results cited above.

The heat flow data described above are too scant and too variable to attempt a generalization. However, the high Lake Whillans value (285 mW/m^2) lies in an unusual tectonic setting (Fig. 1). It lies on the south flank of the WARS adjacent to the TAM, most likely on or near a flanking fault, but more importantly, it lies over the recently discovered slow seismic velocity zone in the uppermost mantle, which overlies a high wave speed root (Shen et al., 2018). This is interpreted to represent foundered lithosphere replaced by warm, low-density asthenosphere that is responsible for uplift of the TAM, and for Miocene volcanism at Mt. Early and Sheridan Bluff, which are far removed from all other centers of Cenozoic volcanism in Antarctica. Licht et al. (2014) describe a third volcanic center 60 km up-glacier from Mt. Early, which adds to the unusual nature of this isolated cluster of volcanic centers. Shen et al. (2018) do not cite Fisher et al. (2015), but high heat flow at this locality is clearly consistent with their findings. Given the unusual (unique?) tectonic setting of the Lake Whillans heat flow value, it seems questionable that this is representative of heat flow values in the WARS as a whole. The remaining three heat flow values noted above fall within the generalized 63-104 mW/m^2 range given for the Basin and Range province by Chapman and Rybach (1985); but whereas the Basin and Range has at least three geothermal systems with >1000 mW/m^2, according to these authors, no such hot springs have been found within the WARS.

Taken together with the seismic and elevation characteristics described above, the interior of the rift (i.e. excluding the MBL dome) appears to lack evidence for a large volume of late Cenozoic volcanic rock beneath the WAIS. This is consistent with the results of the sediment analysis described above.

6. Conclusions

We find no evidence to support the suggestions that Ross Sea glacial drainage system is underlain by an extensive outcrop of late Cenozoic volcanic facies. If that were the case then surface sediments from the Ross Sea should contain significant weight % of minerals such as pyroxene, and olivine, as well as zeolites. The amorphous silica found in many cores could be diatoms, volcanic glass, or the result of overgrinding. We cannot confidently interpret this material as volcanic glass when it is not accompanied by olivine or pyroxene. The results of quantitative X-ray diffraction analyses rather indicated that the samples have large wt%s of quartz, and a sediment unmixing program confirmed that the samples had a close affinity to samples of granite bedrock with only a few samples out of 51 showing any admixture with alkali basalt-derived bedrock.

CRediT authorship contribution statement

This is a joint authored paper. Andrews was responsible for the mineral analyses and LeMasurier was involved with the issues of the bedrock and volcanic history.

Declaration of competing interest

The authors declare that they have no known competing financial interests or personal relationships that could have appeared to influence the work reported in this paper.

Acknowledgements

We thank Valerie Stanley at the Oregon State Core Repository for all her efforts to obtain sediment samples for us and to Dr Anne Grunow at the Polar Rock Repository Ohio State Univ. for obtaining bedrock samples for our use. Dr Kathy Licht provided the samples from the Ross Ice Shelf. Wendy Roth, INSTAAR, is thanked for the supervision of the INSTAAR Sedimentology and XRD Laboratory. We thank Dr. Albert Kettner, our INSTAAR colleague, for help with producing Fig. 1. We are grateful to Gary Clow, of INSTAAR, for permission to cite unpublished heat flow data, for providing all the published heat flow data used here, and for helping with an overview of its implications for the WARS. WEL gratefully acknowledges the support of National Science Foundation grants DPP77-27546, DPP80-20836, and #0536526, administered by the Office of Polar Programs, to study the geology and geochemistry of Marie Byrd Land volcanoes. JTA also acknowledges NSF support for research grants in the 1990's to investigate the glacial history in the Ross Sea and thanks Dr J.B. Anderson and the late Eugene Domack for involving him in Antarctic research. We appreciate the comments of the Editor and the reviews of Dr JL Smellie and an anonymous reviewer.

Appendix A. Supplementary material

Supplementary material related to this article can be found online at https://doi.org/10.1016/j.epsl.2021.117035.

References

Aitchison, J., 1986. The Statistical Analysis of Compositional Data. Chapman and Hall, London.

Alley, R.B., Blankenship, D.D., Rooney, S.T., Bentley, C.R., 1989. Sedimentation beneath ice shelves - the view from ice stream-B. Mar. Geol. 85, 101–120.

Alley, R.B., Cuffey, K.M., Evenson, E.B., Lawson, D.E., Strasser, J.C., 1997. How glaciers entrain and transport basal sediment: physical constraints. Quat. Sci. Rev. 16, 1017–1038.

Anderson, J.B., Bartek, L.R., 1991. Facies distribution resulting from sedimentation under polar interglacial climatic conditions within a high-latitude marginal basin, McMurdo Sound, Antarctica. In: Anderson, J.B., Ashley, G.M. (Eds.), Glacial Marine Sedimentation; Paleoclimatic Significance. Geological Society of America, Boulder, CO, pp. 27–49.

Anderson, J.B., Domack, E.W., Kurtz, D.D., 1980. Observations of sediment-laden icebergs in Antarctic waters: implications to glacial erosion and transport. J. Glaciol. 25, 387–396.

Anderson, J.B., Kennedy, D.S., Smith, M.J., Domack, E.W., 1991. Sedimentary facies associated with Antarctica's floating ice masses. In: Anderson, J.B., A, G.M. (Eds.), Paleoclimatic Interpretation of Glacial Marine Deposits. Geological Society of America, Boulder, pp. 1–125.

Andrews, J.T., 1987. Late Quaternary marine sediment accumulation in fiord-shelf-deep-sea transects, Baffin Island to Baffin Bay. Quat. Sci. Rev. 6, 231–243.

Andrews, J.T., Bjork, A.A., Eberl, D.D., Jennings, A.E., Verplanck, E.P., 2015. Significant differences in late Quaternary bedrock erosion and transportation: East versus West Greenland ~70°N and the evolution of glacial landscapes. J. Quat. Sci. 30, 452–463.

Andrews, J.T., Domack, E.W., Cunningham, W.L., Leventer, A., Licht, K.J., Jull, A.J.T., DeMasters, D.J., Jennings, A.E., 1999. Problems and possible solutions concerning radiocarbon dating of surface marine sediments, Ross Sea, Antarctica. Quat. Res. 52, 206–216.

Andrews, J.T., Eberl, D.D., 2012. Determination of sediment provenance by unmixing the mineralogy of source-area sediments: the "SedUnMix" program. Mar. Geol. 291, 24–33.

Andrews, J.T., Jenner, K., Campbell, C.D., 2020. Linking marine core lithofacies and mineral and grain-size compositions on the Baffin Island margin: changes in provenance and transport. J. Sediment. Res. 90, 1–13.

Andrews, J.T., Jull, A.J.T., Leventer, A., 1997. Replication of accelerator mass spectrometry carbon-14 dates on the acid-insoluble fraction of Ross Sea surface sediments. Antarct. J. US 32 (5), 37–38.

Andrews, J.T., Kristjansdottir, G.B., Eberl, D.D., Jennings, A.E., 2013. A quantitative X-ray diffraction inventory of tephra and volcanic glass inputs into the Holocene marine sediment archives of Iceland: a contribution to V.A.S.T. Polar Res., 1–15.

Andrews, J.T., Tedesco, K., 1992. Detrital carbonate-rich sediments, northwestern Labrador Sea: implications for ice-sheet dynamics and iceberg rafting (Heinrich) events in the North Atlantic. Geology 20, 1087–1090.

Bamber, J.L., Oppenheimer, M., Kopp, R.E., Aspinall, W.P., Cooke, R.M., 2019. Ice sheet contributions to future sea-level rise from structured expert judgement. Proc. Natl. Acad. Sci. USA 116, 11,195–11,200.

Bartek, L.R., Anderson, J.B., 1991. Facies resulting from sedimentation under polar interglacial climatic conditions within a high-latitude marginal basin, McMurdo Sound, Antarctica. In: Anderson, J.B., Ashley, G.M. (Eds.), Glacial Marine Sedimentation; Paleoclimatic Significance. Geological Society of America, Boulder, CO, pp. 27–49.

Behrendt, J.C., 1990. Volcanoes of the Antarctic Plate and Southern Oceans. In: LeMasurier, W.E., Thomson, J.W. (Eds.), A.12. Ross Sea, Antarctic Research Series. American Geophysical Union, Washington, DC, pp. 89–90.

Behrendt, J.C., Bell, R.E., Blankenship, D.D., 1993. Active volcanism beneath the West Antarctic ice sheet and implications for ice-sheet stability. Nature 361, 526.

Bell, M., Laine, E.P., 1985. Erosion of the Laurentide region of North America by glacial and glaciofluvial processes. Quat. Res. 23, 154–174.

Bentley, C.R., Clough, J.W., Robertson, J.D., 1974. Risp geophysical work. Antarct. J. US 9, 157–159.

Blankenship, D.D., Bell, R.E., Hodge, S.M., Brozena, J.M., Behrendt, J.C., Finn, C.A., 1993. Active volcanism beneath the West Antarctic ice-sheet and implications for ice-sheet stability. Nature 361, 526–529.

Boulton, G.S., 1982. Subglacial processes and the development of glacial bedforms. In: Davidson-Arnott, R., Nickling, W., Fahey, B.D. (Eds.), Research in Glacial, Glacio-Fluvial, and Glacio-Lacustrine Systems: Proceedings of the 6th Guelph Symposium on Geomorphology, 1980. Geo Books, University of Guelph, pp. 1–31.

Boulton, G.S., 1996. Theory of glacial erosion, transport and deposition as a consequence of subglacial sediment deformation. J. Glaciol. 42, 43–62.

Boyd, R.W., Piper, D.J.W., 1976. Baffin Bay continental shelf clay mineralogy. Marit. Sediments 21, 17–18.

Brooks, C.K., Nielsen, T.F.D., 1982. The Phanerozoic development of the Kangerdlugssuaq area, East Greenland. Meddelelser on Gronland, Geoscience 9, 1–30.

Chapman, D.S., Rybach, L., 1985. Heat flow anomalies and their interpretation. In: Rybach, L. (Ed.), Heat Flow and Geothermal Processes. J. Geodyn. 4, 3–37.

Chayes, F., 1971. Ratio Correlation. University of Chicago Press, Chicago.

Church, J.A., Clark, P.U., Cazenave, A., Gregory, J.M., Jevrejeva, S., Levermann, A., et al., 2013. Sea level change. In: Climate Change 2013: The Physical Science Basis. Contribution of Working Group 1 to the Fifth Assessment Report of the Intergovernmental Panel on Climate Change. Cambridge University Press, Cambridge, United Kingdom and New York, NY, USA, p. 1535.

Clague, D.A., Davis, A.S., Bischoff, J.L., Dixon, J.E., Geyer, R., 2000. Lava bubble-wall fragments formed by submarine hydrovolcanic explosions on Lo'ihi Seamount and Kilauea Volcano. Bull. Volcanol. 61, 437–449.

Clark, P.U., 1987. Subglacial sediment dispersal and till composition. J. Geol. 95, 527–541.

Corr, H.F.J., Vaughan, D.G., 2008. A recent volcanic eruption beneath the West Antarctic ice sheet. Nat. Geosci. 1, 122–125.

Craddock, C., 1972. Geological Map of Antarctica. The American Geographical Society, New York, NY, p. 10032.

Depoorter, M.A., Bamber, J.L., Griggs, J.A., Lenaerts, J.T.M., Ligtenberg, S.R.M., van den Broeke, M.R., Moholdt, G., 2013. Calving fluxes and basal melt rates of Antarctic ice shelves. Nature 502, 89.

Domack, E.W., Harris, P.T., 1998. A new depositional model for ice shelves, based upon sediment cores from the Ross Sea and the Mac. Robertson shelf, Antarctica. In: Budd, W.F. (Ed.), Ann. Glaciol. 27, 281–284.

Dotto, T.S., Garabato, A.N., Bacon, S., Tsamados, M., Holland, P.R., Hooley, J., Frajka-Williams, E., Ridout, A., Meredith, M.P., 2018. Variability of the Ross Gyre, Southern Ocean: drivers and responses revealed by satellite altimetry. Geophys. Res. Lett. 45, 6195–6204.

Dowdeswell, J.A., Scourse, J.D., 1990. Glacimarine environments: processes and sediments. Geol. Soc. Spec. Publ. 53, 155–176.

Dreimanis, A., 1976. Tills: their origin and properties. In: Legget, R.F. (Ed.), Glacial Till an Inter-Disciplinary Study. The Royal Society of Canada Special Publications, pp. 11–49.

Dreimanis, A., 1984. Lithofacies types and vertical profile, and alternative approach to the description and environmental interpretation of glacial diamict and diamictite. Sedimentology 31, 885.

Drewry, D.J., 1983. Antarctic Ice Sheet: aspects of current configuration and flow. In: Gardner, R., Scoging, H. (Eds.), Mega-Geomorphology. Clarendon Press, Oxford, pp. 18–38.

Drewry, D., 1986. Glacial Geologic Processes. Edward Arnold, London.

Eberl, D.D., 2003. User guide to RockJock: a program for determining quantitative mineralogy from X-ray diffraction data. United States Geological Survey, Open File Report 03-78, Washington, DC, 40 pp.

Ehrmann, W., Hillenbrand, C.-D., Smith, J.A., Graham, A.G.C., Kuhn, G., Larter, R.D., 2011. Provenance changes between recent and glacial-time sediments in the Amundsen Sea embayment, West Antarctica: clay mineral assemblage evidence. Antarct. Sci. 23, 471–486.

Ellerman, P.J., 1992. Depositional environments and post-depositional alteration of Cenozoic hyaloclastites in Antarctica. Unpublished Ph.D. thesis. Department of Geological Sciences, University of Colorado.

Farmer, G.L., Barber, D.C., Andrews, J.T., 2003. Provenance of Late Quaternary ice-proximal sediments in the North Atlantic: Nd, Sr and Pd isotopic evidence. Earth Planet. Sci. Lett. 209, 227–243.
Farmer, G.L., Licht, K.J., 2016. Generation and fate of glacial sediments in the central Transantarctic Mountains based on radiogenic isotopes and implications for reconstructing past ice dynamics. Quat. Sci. Rev. 150, 98–109.
Farmer, G.L., Licht, K.J., Swope, J.R., Andrews, J.T., 2006. Isotopic constraints on the provenance of fine-grained sediment in LGM tills from the Ross Embayment, Antarctica. Earth Planet. Sci. Lett. 249, 90–107.
Fisher, A.T., Mankoff, K.D., Tulaczyk, S.M., Taylor, S.W., Foley, N., the WISSARD Science Team, 2015. High geothermal heat flux measured below the West Antarctic ice sheet. Sci. Adv. 1, e1500093.
Golledge, N.R., Levy, R.H., McKay, R.M., Fogwill, C.J., White, D.A., Graham, A.G.C., Smith, J.A., Hillenbrand, C.D., Licht, K.J., Denton, G.H., Ackert, R.P., Maas, S.M., Hall, B.L., 2013. Glaciology and geological signature of the Last Glacial Maximum Antarctic ice sheet. Quat. Sci. Rev. 75, 225–247.
Hallet, B., Hunter, L., Bogen, J., 1996. Rates of erosion and sediment evacuation by glaciers: a review of field data and their implications. Glob. Planet. Change 12, 213–235.
Hemming, S.R., 2004. Heinrich events: massive late Pleistocene detritus layers of the North Atlantic and their global climate imprint. Rev. Geophys. 42, RG1005/2004.
Honnorez, J., Kirst, P., 1975. Submarine basaltic volcanism: morphometric parameters for discriminating hyaloclastites from hyalotuffs. Bull. Volcanol. 39, 1–25.
Hooke, R.L., Cummings, D.I., Lesemann, J.E., Sharpe, D.R., 2013. Genesis of dispersal plumes in till. Can. J. Earth Sci. 50, 847–855.
Hughes, T., 1975. The West Antarctic Ice Sheet: instability, disintergration, and initiation of ice ages. Rev. Geophys. Space Phys. 13.
Iverson, N.A., Lieb-Lappen, R., Dunbar, N.W., Obbard, R., Kim, E., Golden, E., 2017. The first physical evidence of subglacial volcanism under the West Antarctic Ice Sheet. Sci. Rep. 7. https://doi.org/10.1038/s41598-017-11515-3.
Jennings, A.E., Andrews, J.T., Wilson, L., 2011. Holocene environmental evolution of the SE Greenland Shelf north and south of the Denmark Strait: Irminger and East Greenland current interactions. Quat. Sci. Rev. 30, 980–998.
Jones, J.G., 1966. Intraglacial volcanoes of southwest Iceland and their significance in the interpretation of the form of the marine basaltic volcanoes. Nature 212, 586–588.
Jones, J.G., 1969. Intraglacial volcanoes of the Laugarvatn region, southwest Iceland, I. Q. J. Geol. Soc. Lond. 124, 197–211.
King, C., Hall, B., Hillebrand, T., Stone, J., 2020. Delayed maximum and recession of an East Antarctic outlet glacier. Geology 48, 630–634.
Klassen, R.A., 1993. Glacial history, drift composition, and mineral exploration, central Labrador. Bull., Geol. Surv. Can. 435. 76 pp.
Kopp, R.E., Gilmore, E.A., Little, C.M., Lorenzo-Trueba, J., Ramenzoni, V.C., Sweet, W.V., 2019. Usable science for managing the risks of sea-level rise. Earth's Future 7. https://doi.org/10.1029/2018EF001145.
Kurtz, D.D., Anderson, J.B., 1979. Recognition and sedimentologic description of recent debris flow deposits from the Ross and Weddell Seas, Antarctica. J. Sediment. Petrol. 49, 1159–1170.
Larsen, B., 1983. Geology of the Greenland-Iceland ridge in the Denmark strait. In: Bott, M.H.P., Saxov, S., Talwani, M., Thiede, J. (Eds.), Structure and Development of the Greenland-Scotland Ridge. Plenum Publishing Corp., London, pp. 425–444.
LeMasurier, W.E., 2002. Architecture and evolution of hydrovolcanic deltas in Marie Byrd Land, Antarctica. In: Smellie, J.L., Chapman, M.G. (Eds.), Volcano-Ice Interaction on Earth and Mars. Geol. Soc. (Lond.) Spec. Publ. 202, 115–148.
LeMasurier, W.E., 2008. Neogene extension and basin deepening in the West Antarctic rift inferred from comparisions with the East African rift and other analogs. Geology 36, 247–250.
LeMasurier, W., 2013. Shield volcanoes of Marie Byrd Land, West Antarctic rift: oceanic island similarities, continental signature, and tectonic controls. Bull. Volcanol. 75, 726. https://doi.org/10.1007/s00445-013-0726-1.
LeMasurier, W.E., Rocchi, S., 2005. Terrestrial record of post-Eocene climate history in Marie Byrd Land, West Antarctica. Geogr. Ann. 87A, 51–66.
LeMasurier, W.E., Thomson, J.W.E., 1990. Volcanoes of the Antarctic Plate and Southern Oceans. Antarctic Research Series. American Geophysical Union, Washington, DC, p. 487.
Licht, K.J., 1999. Investigations into the Late Quaternary History of the Ross Sea, Antarctica. Department of Geological Sciences, University of Colorado, Boulder, p. 216.
Licht, K.J., Dunbar, N.W., Andrews, J.T., Jennings, A.E., 1999. Distinguishing subglacial till and glacial marine diamictions in the western Ross Sea, Antarctica: implications for a last glacial maximum grounding line. Geol. Soc. Am. Bull. 111, 91–103.
Licht, K.J., Hemming, S.R., 2017. Analysis of Antarctic glacigenic sediment provenance through geochemical and petrologic applications. Quat. Sci. Rev. 164, 1–24.
Licht, K.J., Hennessy, A.J., Welke, B.M., 2014. The U-Pb detrital zircon signature of West Antarctic ice stream tills in the Ross embayment, with implications for Last Glacial Maximum ice flow reconstructions. Antarct. Sci. 26, 687–697.
Licht, K.J., Lederer, J., Farmer, G.L., Swope, J.R., Andrews, J.T., 2006. Petrographic and isotopic composition of Late Quaternary Ross Embayment till. Terra Antarct. Rep. 12, 35–42.
Licht, K.J., Lederer, J.R., Swope, R.J., 2005. Provenance of LGM glacial till (sand fraction) across the Ross embayment, Antarctica. Quat. Sci. Rev. 24, 1499–1520.
Lloyd, A.J., Wiens, D.A., Nyblade, A.A., Anandakrishnan, S., Aster, R.C., Huerta, A.D., Wilson, T.J., Dalziel, I.W.D., Shore, P.J., Zhao, D., 2015. A seismic transect across West Antarctica: evidence for mantle thermal anomalies beneath the Bentley Subglacial Trench and the Marie Byrd land Dome. J. Geophys. Res., Solid Earth 120. https://doi.org/10.1002/2015JB012455.
McCarty, D.K., 2002. Quantitative mineral analysis of clay-bearing mixtures: the "Reynolds Cup" contest. Int. Union Crystallogr. Newslett. 27, 12–16.
McKay, R., Golledge, N.R., Maas, S., Naish, T., Levy, R., Dunbar, G., Kuhn, G., 2016. Antarctic marine ice-sheet retreat in the Ross Sea during the early Holocene. Geology 44, 7–10.
Mercer, J.H., 1978. West Antarctic ice sheet and CO_2 greenhouse effect: a threat of disaster. Nature 271, 321–325.
Palmer, E.F., Licht, K.J., Swope, R.J., Hemming, S.R., 2012. Nunatak moraines as a repository of what lies beneath the East Antarctic Ice Sheet. Spec. Pap., Geol. Soc. Am. 487, 97–104.
Pereira, P.S., van de Flierdt, T., Hemming, S.R., Hammond, S.J., Kuhn, G., Brachfeld, S., Doherty, C., Hillenbrand, C.-D., 2018. Geochemical fingerprints of glacially eroded bedrock from West Antarctica: detrital thermochronology, radiogenic isotope systematics and trace element geochemistry in Late Holocene glacial-marine sediments. Earth-Sci. Rev. 182, 204–232.
Piper, D.J.W., Slatt, R.M., 1977. Late quaternary clay mineral distribution on the eastern continental margin of Canada. Geol. Soc. Am. Bull. 88, 267–272.
Prest, V.K., 1990. Laurentide ice-flow patterns: a historial review, and implications of the dispersal of Belcher Island erratics. Géogr. Phys. Quat. 44, 113–136.
Raven, M.D., Self, P.G., 2017. Outcomes of 12 years of the Reynolds cup quantitative mineral analysis round Robin. Clays Clay Miner. 65, 122–134.
Ritzwoller, M.H., Shapiro, N.M., Levshin, A.L., Leahy, G.M., 2001. Crustal and upper mantle structure beneath Antarctica and surrounding oceans. J. Geophys. Res. 106, 30,645–30,670.
Rocchi, S., LeMasurier, W.E., DiVincenzo, G., 2006. Oligocene to Holocene erosion and glacial history in Marie Byrd Land, West Antarctica, inferred from exhumation of the Dorrel Rock intrusive complex and from volcano morphologies. Geol. Soc. Am. Bull. 118, 991–1005.
Sarna-Wojcicki, A.M., Bowman, H.R., Meyer, C.E., Russell, P.C., Woodward, M.J., Rowe, J.J.J., Baedecker, P.A., Asaro, F., Michael, H., 1984. Chemical Analyses, Correlations, and Ages of Upper Pliocene and Pleistocene as Layers of East-Central and Southern, California. United States Geological Survey, Washington, DC. 33 pp.
Shapiro, N., Ritzwoller, M., 2004. Inferring surface heat flux distributions guided by a global seismic model: particular application to Antarctica. Earth Planet. Sci. Lett. 223, 213–224.
Shen, W., Wiens, D.A., Stern, T., Anandakrishnan, S., Aster, R.C., Dalziel, I., Hansen, S., Heeszel, D.S., Huerta, A., Nyblade, A., Wilson, T.J., Winberry, J.P., 2018. Seismic evidence for lithospheric foundering beneath the southern Transantarctic Mountains, Antarctica. Geology 46, 71–74.
Shilts, W.W., 1976. Glacial till and mineral exploration. In: Legget, R.F. (Ed.), Glacial Till, pp. 205–223.
Smethie, W.M., Jacobs, S.S., 2005. Circulation and melting under the Ross Ice Shelf: estimates from evolving CFC, salinity and temperature fields in the Ross Sea. Deep-Sea Res. Part I - Oceanogr. Res. Pap. 52, 959–978.
Stokes, C.R., 2018. Geomorphology under ice streams: moving from form to process. Earth Surf. Process. Landf. 43, 85–123.
Syvitski, J.P.M., MacDonald, R.D., 1982. Sediment character and provenance in a complex fjord, Howe Sound, British Columbia. Can. J. Earth Sci. 19, 1025–1044.
Van Wyk De Vries, M., Bingham, R.G., Hein, A.S., 2017. A new volcanic province: an inventory of subglacial volcanoes in West Antarctica. In: Siegert, M.J., Jamieson, S.S.R., Siegert, M.J., Jamieson, S.S.R., White, D.A. (Eds.), Exploration of Subsurface Antarctica: Uncovering Past Changes and Modern Processes. Geol. Soc. (Lond.) Spec. Publ. 461. https://doi.org/10.1144/SP461.7.
Vogel, S.W., Tulaczyk, S., Carter, S., Renne, P., Turrin, P., Grunow, A., 2006. Geologic constraints on the existence and distribution of West Antarctic subglacial volcanism. Geophys. Res. Lett. 33, L23501. https://doi.org/10.1029/2006GL027344.
Wellner, J.S., Scambos, T.A., Domack, E.W., et al., 2019. The Larsen Ice Shelf System, Antarctica (LARISSA): polar systems bound together, changing fast. GSA Today 29, 4–9.
Winberry, J.P., Anandakrishnan, S., 2004. Crustal structure of the West Antarctic rift system and Marie Byrd Land hotspot. Geology 32, 977–980.
Yokoyama, Y., Anderson, J.B., Yamane, M., Simkins, L.M., Miyairi, Y., Yamazaki, T., Koizumi, M., Suga, H., Kusahara, K., Prothro, L., Hasumi, H., Southon, J.R., Ohkouchi, N., 2016. Widespread collapse of the Ross Ice Shelf during the late Holocene. Proc. Natl. Acad. Sci. USA 113, 2354–2359.